

STUDY OF FLUID FLOW THROUGH A TUBE WITH AND WITHOUT OBSTACLE

By
Mohammed Mainul Hossain
Roll No: 1009093003, Registration No: 960139
Session: October 2009

Master of Philosophy
In
Mathematics



Department of Mathematics
Bangladesh University of Engineering and Technology
Dhaka-1000, Bangladesh
November-2015

STUDY OF FLUID FLOW THROUGH A TUBE WITH AND WITHOUT OBSTACLE

A dissertation submitted in partial fulfillment of the requirements for the award of the degree

Of
Master of Philosophy
In
Mathematics

By
Mohammed Mainul Hossain
Roll No: 1009093003, Registration No: 960139
Session: October 2009
Department of Mathematics
Bangladesh University of Engineering and Technology
Dhaka-1000, Bangladesh

Supervised by
Dr. Md. Abdul Hakim Khan
Professor
Department of Mathematics, BUET



Department of Mathematics
Bangladesh University of Engineering and Technology
Dhaka-1000, Bangladesh
November-2015

The Thesis entitled
**STUDY OF FLUID FLOW THROUGH A TUBE WITH AND
WITHOUT OBSTACLE**

Submitted By

Mohammed Mainul Hossain

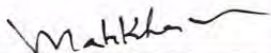
Roll No: 1009093003 (Part time), Registration No: 960139, Session: October 2009.


has been accepted as satisfactory in partial fulfillment of the requirement for the degree of

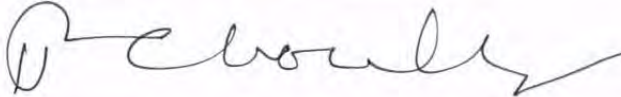
Master of Philosophy in Mathematics

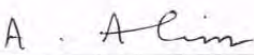
on 29th November 2015.

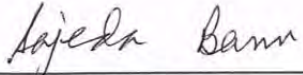
Board of Examiners

1. 

Dr. Md. Abdul Hakim Khan (Supervisor) **Chairman**
Professor
Department of Mathematics, BUET, Dhaka.
2. 

Head **Member**
Department of Mathematics, BUET, Dhaka.
3. 

Dr. Md. Mustafa Kamal Chowdhury **Member**
Professor
Department of Mathematics, BUET, Dhaka.
4. 

Dr. Md. Abdul Alim **Member**
Professor
Department of Mathematics, BUET, Dhaka.
5. 

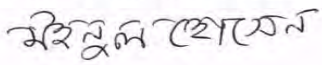
Mrs. Sajeda Banu **Member**
Professor **(External)**
Department of Mathematics, University of Dhaka, Dhaka

Author's Declaration

I declare that the work in this dissertation has carried out in accordance with the Regulation of Bangladesh University of Engineering and Technology, Dhaka. The work is original except where indicated by special reference in the text and no part of it has been submitted for any other degree.

The dissertation has not been presented to any other university for examination either in Bangladesh or overseas.

Name : Mohammed Mainul Hossain

Signature: 

Date: 29/11/15

Acknowledgements

At first all praise belongs to “The Almighty ALLAH”, the most merciful, generous to men and His creation.

I would like to express heartiest gratitude to my supervisor Dr. Md. Abdul Hakim Khan, Professor, Department of Mathematics, BUET, Dhaka, for his good guidance, support, valuable suggestions, constant inspiration and supervision during the research work of the M. Phil. Program. I am highly grateful to him for every effort that he made to get me on the right track of the thesis; otherwise this study would never see the light of day.

I wish to express my gratitude to Prof. Dr. Abdul Alim, Head, Department of Mathematics, BUET, Dhaka, for his encouraging advice and guideline that support me during the M. Phil. course. He also provided all department facilities available that enabled me to work in a comfortable atmosphere. I am really indebted to him.

I express my deep regards to Prof. Dr. Md. Mustafa Kamal Chowdhury, the former Head, Department of Mathematics, BUET, Dhaka, for his wise and liberal cooperation during my course of M. Phil. program.

I wish to express my gratitude to Prof. Dr. Manirul Alam Sarker, Professor, Department of Mathematics, BUET, Dhaka, for his valuable and necessary help during my course work. His advice on my research always inspires me.

I would like to extend my sincere thanks to all other respected teachers of this department for their valuable comment and inspiration throughout my M. Phil. Program.

Certainly, I am deeply indebted to my parents from whom I have learned the best things needed for life. They guided me through the entire studies and helped me morally and spiritually. I am also grateful to my wife, without help of her it is impossible for me to complete the course successfully.

Abstract

The study of fluid flows through tube has received considerable attention over few centuries due to its wide applications in physical, biological and applied sciences. It is therefore necessary to examine some combined effects on the entire flow structure. In this thesis, three different circumstances of fluid flow through a tube are studied. In this regard, wall driven flow through a porous tube with magnetic field and flow through a collapsible tube in presence of obstacle and magnetic field are considered. A numerical study of two-dimensional, steady as well as unsteady flow of an incompressible viscous fluid are investigated using approximation method and finite element method. To determine the stability of flow is main concern. In this thesis, different types of disturbance such as movement of wall, porosity in wall, contraction and expansion of collapsible tube, magnetic field and obstacle are used that help to create instability in flow structure. Special type of Hermite-Padé approximation method is used to analyze the stability of flow and to determine the critical point where the instability initiates. The effect of different dimensionless numbers on the velocity, temperature and rate of heat transfer are also investigated. Here, the critical Reynolds number, effect of contraction and expansion, formation of vortex and magnetic effect on vortex are discussed.

Contents

Board of Examiners
Author's Declaration
Acknowledgements
Abstract
Nomenclature
List of Tables
List of Figures

	Page
1. Overview	
1.1 Introduction	1
1.1 Literature Review	2
1.2 Objective of the Thesis	5
1.3 Outline of the Thesis	5
2. MHD effect on fluid flow and heat transfer through a porous tube	
2.1 Introduction	6
2.2 Mathematical Formulation	6
2.3 Comparison of Series Solution	12
2.4 Result and Discussion	13
2.4.1 Stability Analysis	13
2.4.2 Hydro magnetic Effect	15
2.5 Conclusion	17
3. MHD effect on fluid flow and heat transfer through a collapsible tube	
3.1 Introduction	18
3.2 Physical Model	18
3.3 Comparison of Series Solution	23
3.4 Result and Discussion	25
3.4.1 Stability Analysis	25
3.4.2 Effect of Magnetic Field on Critical Reynolds Number	26
3.4.3 Effect of Magnetic Field on Velocity and Temperature	27
3.5 Conclusion	30
4. MHD effect on fluid flow and heat transfer through a collapsible tube with obstacle and without obstacle	
4.1 Introduction	31
4.2 Physical Model	32

4.3	Governing Equations	32
4.4	Dimensionless Analysis	34
4.5	Finite Element Formulation and Computation	35
4.6	Result and Discussion	37
4.6.1	Velocity Profile of Collapsible Tube	37
4.6.2	Effect of Obstacle on Collapsible Tube	37
4.6.3	Effect of Hartmann Number on Heat Transfer	40
4.6.4	Effect of Reynolds Number on Temperature	40
4.6.5	Effect of Reynolds Number on Vortex	43
4.6.6	Effect of Hartmann Number on Vortex	45
4.7	Conclusion	48
5.	Conclusion	49
	References	51

Nomenclature

a	Characteristic radius of the tube
E	Characteristic velocity
B_0	Magnetic induction along the normal of the tube axis
u	Velocity along the z axis
v	Velocity along the r axis
T_0	Fluid temperature
T_w	Wall temperature
ρ	Density of the fluid
P	Pressure
T	Temperature
ν	Kinematic viscosity
κ	Thermal conductivity
C_P	Specific heat capacity
Ψ	Stream function
ω	Vorticity
Re	Reynolds number
Ha	Hartmann number
Pr	Prandtl number
α	Rate of contraction and expansion
a_0	Initial radius of collapsible tube
η	Dimensionless radius
U_0	Initial velocity
D	Diameter of the tube
d_c	Depth of contraction, expansion and width of obstacle

List of Tables

Tables	Page
Table 2.1: Critical Reynolds number and convergence of series	13
Table 2.2: Magnetic effect on the critical Reynolds number	15
Table 3.1: Critical Reynolds number and critical exponent	25
Table 3.2: Magnetic effect on critical Reynolds number	26
Table 4.1: Grid sensitivity test (where $Re = 100, Pr = 0.71, Ha = 10$).	36

List of Figures

Figures	Page
Figure 2.1: Temperature distribution for $(Re = 1, Pr = 7.1)$, $(Re = 1, Pr = 1.0)$ and $(Re = 1, Pr = 0.71)$	12
Figure 2.2: Temperature distribution for $(Pr = 7.1, Re = 1.5)$, $(Pr = 7.1, Re = 1.0)$ and $(Pr = 7.1, Re = 0.5)$	12
Figure 2.3: The wall shear stress $G(1)$ versus Reynolds number	12
Figure 2.4: Rate of heat transfer versus Reynolds number $(Pr = 7.1, Pr = 1.0, Pr = 0.71)$	12
Figure 2.5 (a): Shear stress versus Reynolds number for $(d = 2, Ha = 0)$	13
Figure 2.5 (b): Shear stress versus Reynolds number for $(d = 3, Ha = 0)$	13
Figure 2.5 (c): Shear stress versus Reynolds number for $(d = 4, Ha = 0)$	14
Figure 2.6: Velocity versus distance from center for different Reynolds number $(Ha = 0, Re = 1)$, $(Ha = 0, Re = 2)$, $(Ha = 0, Re = 2.1)$	14
Figure 2.7: Shear stress versus Reynolds number for different Magnetic field values $(Ha = 0, Ha = 1, Ha = 2)$	15
Figure 2.8: Velocity versus distance from center for different Magnetic field values $(Ha = 0, Ha = 2, Ha = 2.5)$	16
Figure 2.9: Temperature versus distance from center for different Magnetic field values $(Ha = 0, Re = 1, Pr = 0.71)$, $(Ha = 2, Re = 1, Pr = 0.71)$, $(Ha = 3, Re = 1, Pr = 0.71)$	16
Figure 2.10: Nusselt number versus Magnetic field intensity $(Re = 1, Pr = 0.71)$	17
Figure 3.1: Temperature profile for different Prandtl number $(Pr > 1)$ and $(Pr = 7.1, Re = 1)$, $(Pr = 4, Re = 1)$, $(Pr = .71, Re = 1)$	23
Figure 3.2: Temperature profile for different Prandtl number $(Pr < 1)$ and $(Pr = 0.1, Pr = 0.2, Pr = 0.3)$	23
Figure 3.3: Temperature profile for different Reynolds number $(Re = 1.5, Pr = 1)$, $(Re = 1.0, Pr = 1)$, $(Re = 0.5, Pr = 1)$	23

Figure 3.4: Nusselt number versus Reynolds number for ($Pr = 1, Pr = 2, Pr = 3$)	23
Figure 3.5: Nusselt number versus Reynolds number for ($Pr = 3.0, Pr = 2.0, Pr = 1.0$)	24
Figure 3.6: Velocity profile for different Reynolds number for ($Re = 1.0, Re = 5.0, Re = 7.0$)	24
Figure 3.7: Shear stress versus Reynolds number for ($Ha = 0$)	25
Figure 3.8: Velocity versus distance from center for different Reynolds number ($Ha = 0, Re = 1.5$), ($Ha = 0, Re = 2.2$)	26
Figure 3.9: Shear stress versus Reynolds number for different Magnetic field values ($Ha = 0, Ha = 1, Ha = 2, Ha = 3$)	27
Figure 3.10: Velocity versus distance from center for different Magnetic field parameter ($Ha = 0, Re = 1$), ($Ha = 2, Re = 1$), ($Ha = 3, Re = 1$)	27
Figure 3.11: Temperature versus Prandtl number ($Ha = 0, Re = 1$)	28
Figure 3.12: Temperature versus distance from center for different Magnetic field parameter ($Ha = 0, Re = 1, Pr = 0.71$), ($Ha = 2, Re = 1, Pr = 0.71$), ($Ha = 3, Re = 1, Pr = 0.71$)	28
Figure 3.13: Temperature versus distance from center for different Magnetic field parameter ($Ha = 0, Re = 1, Pr = 7.1$), ($Ha = 2, Re = 1, Pr = 7.1$), ($Ha = 3, Re = 1, Pr = 7.1$)	29
Figure 3.14: Nusselt number versus Hartmann number for ($Re = 1, Pr = 0.71$)	29
Figure 3.15: Nusselt number versus Hartmann number for ($Re = 1, Pr = 7.1$)	30
Figure 4.1(a): Nusselt number versus mesh of the elements for ($Re = 100, Pr = 0.71, Ha = 10$)	36
Figure 4.1(b): Average Temperature versus mesh of the elements for ($Re = 100, Pr = 0.71, Ha = 10$)	36
Figure 4.2 (a): Velocity versus radius of the tube for different Reynolds number ($Ha = 0, Re = 1$), ($Ha = 0, Re = 10$), ($Ha = 0, Re = 40$)	37
Figure 4.2 (a): Velocity versus radius of the tube for different Hartmann number ($Ha = 0, Re = 10$), ($Ha = 10, Re = 10$), ($Ha = 20, Re = 10$)	37

Figure 4.3: Velocity versus Reynolds number for obstacle and without obstacle ($Ha = 0$)	37
Figure 4.4: Temperature versus Reynolds number for obstacle and without obstacle at ($Ha = 0, Pr = 0.71$)	38
Figure 4.5: Rate of heat transfer versus Reynolds number for obstacle and without obstacle at ($Ha = 0, Pr = 0.71$)	38
Figure 4.6: Temperature versus Hartmann number for obstacle and without obstacle at ($Re = 1, Pr = 0.71$)	39
Figure 4.7: Rate of Heat transfer versus Hartmann number for obstacle and without obstacle at ($Re = 1, Pr = 0.71$)	39
Figure 4.8: Rate of heat transfer versus Hartmann number with obstacle in air and water ($Pr = .71$ and 7.1)	40
Figure 4.9 (a): Isothermal line on a collapsible tube without obstacle at $Re = 1, Pr = 0.71, Ha = 0$	40
Figure 4.9 (b): Isothermal line on a collapsible tube with obstacle at $Re = 1, Pr = 0.71, Ha = 0$	41
Figure 4.9 (c): Isothermal line at $Re = 10, Pr = 0.71, Ha = 0$ on a collapsible tube without obstacle.	41
Figure 4.9 (d): Isothermal line on a collapsible tube with obstacle at $Re = 10, Pr = 0.71, Ha = 0$	41
Figure 4.9 (e): Isothermal line on a collapsible tube without obstacle at $Re = 40, Pr = 0.71, Ha = 0$	42
Figure 4.9 (f): Isothermal line on a collapsible tube with obstacle at $Re = 40, Pr = 0.71, Ha = 0$	42
Figure 4.10 (a): Stream line on a collapsible tube with obstacle at $Re = 100, Ha = 0$	43
Figure 4.10 (b): Stream line on a collapsible tube with obstacle at $Re = 200, Ha = 0$	43
Figure 4.10 (c): Stream line on a collapsible tube with obstacle at $Re = 300, Ha = 0$	43
Figure 4.10 (d): Stream line on a collapsible tube with obstacle at $Re = 400, Ha = 0$	44

Figure 4.11: Vortex center distance from the obstacle versus Reynolds number	44
Figure 4.12: Vortex length from the obstacle versus Reynolds number	45
Figure 4.13(a): Stream line on a tube with obstacle at $Re = 400, Ha = 0$	45
Figure 4.13(b): Stream line on a tube with obstacle at $Re = 400, Ha = 20$	46
Figure 4.13(c): Stream line on a tube with obstacle at $Re = 400, Ha = 40$	46
Figure 4.13(d): Stream line on a tube with obstacle at $Re = 400, Ha = 60$	46
Figure 4.13(e): Stream line on a tube with obstacle at $Re = 400, Ha = 80$	47
Figure 4.14: Vortex center distance from the obstacle versus Hartman number.	47
Figure 4.15: Vortex length from the obstacle versus Hartmann number.	48

Chapter 1

Overview

1.1 INTRODUCTION

A fluid is any substance that deforms continuously when subjected to a shear stress (tangential force per unit area), no matter how small according to McDonough. The work of Leonardo Da Vinci gave rapid advancement to the study of fluid mechanics more than 500 years ago, but earlier than this time; fluid behavior were much more available by the time of ancient Egyptian. Enough practical information had been gathered during the Roman Empire to allow fluid dynamics application. Several centuries ago, more modern understanding of fluids motion was begun that known as Bernoulli's equation. Since then, many researchers have done numerous works on fluid mechanics.

The study of fluid flows and heat transfer through a porous tube fascinated mankind for many centuries due to its applications in many areas of life. Such areas are: agriculture (e.g. irrigation, land drainage), geothermal system, micro-electric heat transfer equipment, coal and grain storage, nuclear waste disposal, hydraulic engineering, atmospheric sciences, oceanography, geophysics (e.g. convection in the earth's mantle, convection in earth's molten core). So also in a chemical and petroleum engineering (e.g. industrial filtration, fluidization, sedimentation, metallurgy, ceramics, powders, drying and wetting of textiles and wood), building engineering (e.g. aeration insulation against moisture) and biological area (e.g. flow of blood and water in the system, action of kidney and rise of juices in plant).

While the flow over a circular cylinder represents one of the classical problems in fluid mechanics, the case of flow over a confined cylinder in a plane channel remains relatively unexplored. The extra confinement provided by the stationary no-slip walls of the channel affects the nature and stability of the flow. To understand the wide variety of flow phenomena it is very important to gather overall knowledge on bluff body (obstacle) in fluid dynamics. Even more importantly, such a flow configuration represents an idealization of several industrially important flows, where flow inserts can be used to enhance mixing and heat transfer; typical examples include flow past dividers in polymer processing, turbulence promoters in the liquid-metal blankets of fusion reactors, etc. Understanding the dynamics of a three dimensional wake flow behind a cylinder can provide valuable knowledge with practical importance, with respect to its effect on heat and mass transfer.

However, the flow of an electrically conducting viscous fluid between two parallel plates in the presence of a transversely applied magnetic field has applications in many devices such as magneto-hydrodynamic (MHD) power generators, MHD pumps, accelerators, aerodynamics heating, electrostatic precipitation, polymer technology, petroleum industry, purification of

molten metal's from non-metallic inclusions and fluid droplets-sprays. Hartmann flow of a Newtonian fluid with heat transfer, subjected to different physical effects, has been studied by many authors. These results are important for the design of the duct wall and the cooling arrangements. The rectangular channel problem has later been extended also to fluids obeying non-Newtonian constitutive equations. The hydrodynamic flow of a visco-elastic fluid has attracted the attention of many authors due to its important industrial applications.

In this thesis, analysis of MHD flow is major concerned on three different situations. The wall driven flow through porous tube, flow through collapsible tube and flow through collapsible tube with obstacle in the presence of hydro-magnetic effect are studied.

1.2 LITERATURE REVIEW

MHD effect on wall driven flow and heat transfer through a tube with porous wall is the first problem of this thesis. The study of fluid flows in porous tube and channel have received considerable attention over few centuries due to its wide applications in physical, biological and applied sciences. Berman (1953) studied laminar flow in a two dimensional rectangular channel with porous wall. He showed the corresponding Navier-Stoke equations can be reduced to a nonlinear third order ordinary differential equation with two point boundary conditions and Reynolds number (Re) based on injection-velocity. The perturbation results for extremely small Reynolds number was given by him. Some years later, Sellar (1955) obtained a solution for large Reynolds number. However, Yuan and Finkelstein (1956) obtained solution for large negative Reynolds number. Makinde (1995) investigated the problem of laminar flow in channels of slow varying width and permeable boundaries. Makinde (1996) considered the computer extension of perturbation series solution, its analysis and analytic continuation provided valuable information on the solution structure at large Reynolds numbers, including bifurcation study for porous tube flow problem. Makinde (1999) investigated a new series summation and converging improvement technique to study the steady flow of a viscous incompressible fluid flow both in a porous pipe with moving walls and an exponentially diverging asymmetrical channel. Munson-McGee (2002) presented an approximate solution for fluid dynamics of flow through a porous tube, where he encountered in the cross-flow filtration process.

Kays and Crawford (1993) considered heat transfer in a developed laminar incompressible flow with constant physical properties in a two-dimensional channel with porous walls having constant temperature. They obtained several asymptotic solutions of the energy equation for small and large wall Peclet numbers and large Prandtl numbers. Makinde (2001) investigated the combined effects of viscosity variation and energy dissipation on steady flow of an incompressible fluid in a pipe with moving surface. Reddy et al. (2009) observed the unsteady MHD convective heat and mass transfer flow past a semi-infinite vertical porous plate with variable viscosity and thermal conductivity. Makinde (2009) examined the effect of thermal radiation on inherent irreversible in the flow of a variable viscosity optically thin fluid through a channel with isothermal walls. Many investigations have been conducted on thermal stability and heat transfer in a porous channel.

An incompressible symmetric wall driven steady flow of a viscous fluid and heat transfer in a tube of circular cross section was examined by Makinde et al. (2006). They used a perturbation series for the slow flow and low Reynolds number to solve the governing equations. They represented the behavior of wall shear stress and the rate of heat transfer across the wall with the increase or decrease of Reynolds number.

In this thesis, the first problem is solved by the series solution and approximation technique where MHD effect on stability of flow, velocity, shear stress and temperature is represented with the variation of Hartmann number, Reynolds number and Prandtl number.

However, MHD effect on fluid flow and heat transfer through a collapsible tube is the second problem of this thesis. Fluid flow through collapsible tubes is a complex problem due to the interaction between the tube-wall and the flowing fluid, Heil (1997). Collapsible tubes are easily deformed by negative transverse pressure owing to marked reduction of rigidity. Thus, they show a considerable nonlinearity and reveal various complicated phenomena. It is usually used to simulate biological flows such as blood flow in arteries or veins, flow of urine in urethras and airflow in the bronchial airways. These investigations are very useful for the study and prediction of many diseases, as the lung disease (asthma and emphysema), or the cardiovascular diseases (heart stroke). The major research goal remains, the full understanding of the flow structure and the mechanism driving this flow. Many previous theoretical works on flow in collapsible tubes concentrated on the development and analysis of simpler models, by reducing the spatial dimension of the problem, which involved a number of ad-hoc assumptions e.g., Contrad (1969), Grotberg (1971), Flaherty et al. (1972), Cowley (1982,1983) etc. Experimental example of the work on collapsible tube and finite-length elastic tube were performed whose upstream and downstream ends were open (i.e. Starling-resistor), Brower and Scholten (1975), Bertram (1986). Inside a pressure chamber, thin-walled elastic tube (made of latex rubber) was mounted on two rigid tubes. Fluid (liquid or gas) typically water or air respectively was driven through the tube, either by applying a controlled pressure-drop between the ends of the rigid tubes or by controlling the flow rate. At sufficiently large Reynolds numbers, the system produced self-excited oscillations, and exhibited hysteresis in transition between dynamical states, multiple modes of oscillations (each having distinct frequency range), rich and complex nonlinear dynamics (Bertram et al., 1990). If the external pressure exceeds the fluid pressure by a sufficiently large amount, the tube buckles non-axisymmetrically, which then leads to a nonlinear relation between pressure-drop and flow rate. The inertia and resistance of the fluid in the supporting rigid tubes have an important influence on the system's overall dynamics. Meanwhile, Bertram and Pedley (1982), Bertram et al. (1990) investigated two-dimensional channel theoretical model with one wall of the channel was replaced by a membrane under longitudinal tension and viscous flow was driven through the channel by an imposed pressure-drop. The variation between the external pressure and the internal flow was determined the deformation of the membrane. The dynamics of the problem was described by nonlinear ODE's whose numerical solutions exhibited oscillatory behavior in this experiment. Despite the difficulties of producing two-dimensional flows experimentally, this system still attracted considerable theoretical attentions.

Meanwhile, Makinde et al. (2002) investigated the mathematical model of physical phenomena in nonlinear equations for some unknown function. The solutions of these nonlinear systems were dominated by their singularities. Physically, a real singularity controls the behaviour of a solution. There is a long tradition in applied mathematics to solve nonlinear problems by expansion in powers of some “small” perturbation parameter. The advantage of this approach is that it reduces the original nonlinear problem to a sequence of linear problems. However, it is not always possible to find an unlimited number of terms of power series. Often it is possible to obtain a finite number of terms of that series and these may contain a remarkable amount of information. One can reveal the solution behaviour near the critical points by analysing partial sum (Makinde, 2001). Over the last quarter century, highly specialised techniques have been developed to improve the series summation and also used to extract the required information of the singularities from a finite number of series coefficients. The most frequently used methods include Domb and Sykes (1957), Shafer (1974), Hunter and Guerrieri (1980), Sergeev (1986), Drazin and Tourigny (1996) etc.

Makinde (2005) investigated the flow of a viscous incompressible fluid in a collapsible tube. A special type of Hermite-Padé approximants technique was presented and utilized to analyze the flow structure. The chief merit of this new method was its ability to reveal the dominant singularity in the flow field together with solution branches of the underlying problem in addition to the one represented by the original series. Odejide et al. (2008) examined an incompressible viscous fluid flow and heat transfer in a collapsible tube. They investigated on the change in Prandtl number that led to the change in the rate of heat transfer.

In this thesis, the second problem is solved by the series solution and approximation technique where the MHD effect on collapsible tube is represented and compares it with the behavior of normal tube.

Moreover, the MHD effect of fluid flow and heat transfer through a collapsible tube with obstacle is the third problem of my thesis. Flow through collapsible tube with obstacle is an important research area due to its wide range of biological and engineering applications. Although, the geometry of a bluff body (obstacle) can be simple, the flow behind it is chaotic and time-dependent after a certain value of Reynolds number. Forces acting on the body also vary in time, and can cause periodic loading on the body. These forces originate from momentum transfer from fluid to the body, and they are strongly related to the shape of the body and properties of the flow. It was experimentally investigated by Norberg (1987) that when Reynolds number (Re) of flow over a circular cylinder exceeded 48, vortices separated from the boundary layer, and started to move through the downstream, where steady state behavior of the flow turned into a time-dependent state. Also, the flow over a three-dimensional (3D) circular cylinder was analyzed by Aradag (2009) using Large Eddy Simulation (LES) without a sub grid turbulence modeling, where CD and St number were evaluated as 1.2 and 0.2 respectively. The dynamical and thermal behavior of the flow around a circular cylinder submitted to blowing was experimentally investigated by Mathelin et al. (2005).

In this thesis, the MHD effect on fluid flow through a collapsible tube with the presence of obstacle is represented by the variation of stream line, temperature contour, velocity contour

and the rate of heat transfer. However, the deviation of velocity and temperature by the increase and decrease of Reynolds and Hartmann number are studied.

1.3 OBJECTIVE OF THE THESIS

The objective of this thesis is to investigate the flow through a tube with different circumstances. Here, we mainly investigate the presence of magnetic field and obstacle how changes the flow pattern, velocity profile, temperature and rate of heat transfer. The specific objectives are described below.

To develop mathematical model on wall driven flow and collapsible tube with obstacle and hydro magnetic effect using approximation method and finite element method. To compare the result of collapsible tube with normal tube hence to determine the critical Reynolds number for stability and the effect of magnetic field on flow stability. To study the effect of contraction and expansion on velocity, temperature and rate of heat transfer and the presence of obstacle how change the velocity, temperature and rate of heat transfer. Also discuss the magnetic effect on vortex formation, diminish and displacement.

1.4 OUTLINE OF THE THESIS

In this thesis, the fluid flow through a tube is represented with different situations where presence of magnetic field and obstacle is the main focused area.

In Chapter 2, MHD effects on wall driven flow and heat transfer through a porous tube is presented. A mathematical model is developed and the problem is solved by the approximation method and perturbation method. The magnetic effect on velocity, temperature, rate of heat transfer and above all the stability of flow are illustrated.

In Chapter 3, MHD effects on fluid flow and heat transfer through a collapsible tube is described. This problem is solved by the approximation method. The behavior of collapsible tube is compare with the normal tube. The MHD effect on fluid flow, temperature, rate of heat transfer and the stability of flow are demonstrated.

In Chapter 4, MHD flow through a collapsible tube with and without obstacle is discussed and solved using finite element method. The effect of dimensionless number on velocity, temperature and rate of heat transfer in collapsible tube with and without obstacle are discussed. The effect of obstacle and magnetic field on stream line, isothermal line, vortex formation, diminish and its displacement is presented.

Chapter 2

MHD effect on wall driven flow and heat transfer through a porous tube

2.1 INTRODUCTION

Wall driven flow of a viscous fluid with heat transfer and an externally applied homogeneous magnetic field through a two-dimensional symmetrical porous tube of circular cross-section is investigated. Analytical solutions are constructed for the governing nonlinear boundary-value problem using series solution and approximation method based on computer extended series solution and the important properties of the overall flow structure are discussed.

The study of the flow of a viscous fluid through tube of circular cross section is very common in industrial and biological systems. This flow has been considered by many researchers due to its wide area of applications such as oil industries, blood flow in veins, gaseous diffusion in binary mixtures, natural transpiration and cooling etc. Several authors eg Berman (1953), Makinde (1996), Makinde (2001), Makinde et al. (2006), Odejide and Aregbesola (2006) etc. have investigated the flow through different channel with different geometries under various situations.

In this work, wall driven flow of an incompressible viscous fluid through a porous tube of circular cross section in the presence of hydro-magnetic field is considered. Our objectives are to study the hydro-magnetic effect on velocity profile, temperature profile, shear stress and rate of heat transfer through the wall and examine the effect of different dimensionless number. The mathematical formulation of the problem is established and the graphical interpretation of the result is presented.

2.2 MATHEMATICAL FORMULATION

Consider laminar flow of an incompressible viscous fluid through a uniformly porous tube of circular cross section. A polar coordinate system r, z is taken where oz lies along the center of the tube, r is the radial distance. Let u and v be the velocity components in the directions of length and radius of tube respectively, B_0 is the induction of magnetic field that applied along the length of tube. a is the characterize radius. Characterizes the axial wall velocity is E as shown in Figure -2.0.

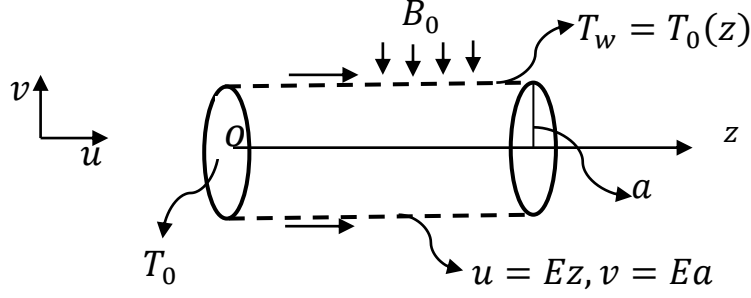


Figure 2.0: Geometry of the problem

The continuity, momentum and energy equations for axisymmetric steady incompressible viscous flow are:

$$\frac{\partial(rv)}{\partial r} + r \frac{\partial u}{\partial z} = 0 \quad (2.1)$$

$$u \frac{\partial u}{\partial z} + v \frac{\partial u}{\partial r} = -\frac{1}{\rho} \frac{\partial P}{\partial z} + \nu(\nabla^2 u) - B_0^2 \frac{\sigma}{\rho} u \quad (2.2)$$

$$u \frac{\partial v}{\partial z} + v \frac{\partial v}{\partial r} = -\frac{1}{\rho} \frac{\partial P}{\partial r} + \nu \left(\nabla^2 v - \frac{v}{r^2} \right) \quad (2.3)$$

$$\rho C_p \left(u \frac{\partial T}{\partial z} + v \frac{\partial T}{\partial r} \right) = \kappa \nabla^2 T \quad (2.4)$$

Where, $\nabla^2 = \frac{\partial^2}{\partial r^2} + \frac{1}{r} \frac{\partial}{\partial r} + \frac{\partial^2}{\partial z^2}$, P is the pressure, T is the temperature, ρ the density, ν the kinematic viscosity of the fluid, κ thermal conductivity, C_p the specific heat capacity at constant pressure, σ electric conductivity and B_0 the induction of magnetic field.

The boundary conditions are:

Along z-axis

$$\frac{\partial u}{\partial r} = 0, \quad v = 0, \quad \frac{\partial T}{\partial r} = 0 \quad \text{on} \quad r = 0 \quad (2.5)$$

The axial velocity, the normal velocity as well as temperature at the wall are

$$u = Ez, \quad v = Ea, \quad T_w = T_0 \left(1 + \frac{z}{a} \right) \quad \text{on} \quad r = a \quad (2.6)$$

where T_0 is the reference temperature at the center and E is constant parameter for characterizing the wall velocity.

Introducing the stream function Ψ and vorticity ω as follows:

$$u = \frac{1}{r} \left(\frac{\partial \Psi}{\partial r} \right) \quad v = -\frac{1}{r} \left(\frac{\partial \Psi}{\partial z} \right) \quad (2.7)$$

$$\omega = \frac{\partial v}{\partial z} - \frac{\partial u}{\partial r} = -\frac{1}{r} \frac{\partial^2 \Psi}{\partial z^2} - \frac{1}{r} \frac{\partial^2 \Psi}{\partial r^2} + \frac{1}{r^2} \frac{\partial \Psi}{\partial r} \quad (2.8)$$

Eliminating pressure P from (2.2) and (2.3) by using (2.7), (2.8) we have

$$\frac{1}{r} \left(\frac{\partial \Psi}{\partial r} \frac{\partial \omega}{\partial z} - \frac{\partial \Psi}{\partial z} \frac{\partial \omega}{\partial r} \right) + \frac{\omega}{r^2} \frac{\partial \Psi}{\partial z} - \frac{B_0^2 \sigma}{\rho} \frac{\partial}{\partial r} \left(\frac{1}{r} \frac{\partial \Psi}{\partial r} \right) = \nu \left(\nabla^2 \omega - \frac{\omega}{r^2} \right) \quad (2.9)$$

Also using (2.7) in (2.4), we obtain

$$\rho C_P \frac{1}{r} \left(\frac{\partial \Psi}{\partial r} \frac{\partial T}{\partial z} - \frac{\partial \Psi}{\partial z} \frac{\partial T}{\partial r} \right) = \kappa \nabla^2 T \quad (2.10)$$

Introducing the following dimensionless variables

$$\bar{\omega} = \frac{\omega}{E}, \quad \bar{z} = \frac{z}{a}, \quad \bar{r} = \frac{r}{a}, \quad \bar{\Psi} = \frac{\Psi}{E a^3}, \quad \bar{T} = \frac{T}{T_0} \quad (2.11)$$

We have

$$Re \left[\frac{1}{\bar{r}} \left(\frac{\partial \bar{\Psi}}{\partial \bar{r}} \frac{\partial \bar{\omega}}{\partial \bar{z}} - \frac{\partial \bar{\Psi}}{\partial \bar{z}} \frac{\partial \bar{\omega}}{\partial \bar{r}} \right) + \frac{\bar{\omega}}{\bar{r}^2} \frac{\partial \bar{\Psi}}{\partial \bar{z}} - Ha^2 \frac{\partial}{\partial \bar{r}} \left(\frac{1}{\bar{r}} \frac{\partial \bar{\Psi}}{\partial \bar{r}} \right) \right] = \nabla^2 \bar{\omega} - \frac{\bar{\omega}}{\bar{r}^2} \quad (2.12)$$

$$Pr Re \left[\frac{1}{\bar{r}} \left(\frac{\partial \bar{\Psi}}{\partial \bar{r}} \frac{\partial \bar{T}}{\partial \bar{z}} - \frac{\partial \bar{\Psi}}{\partial \bar{z}} \frac{\partial \bar{T}}{\partial \bar{r}} \right) \right] = \nabla^2 \bar{T} \quad (2.13)$$

Where $Re = \frac{E a^2}{\nu}$ is the flow Reynolds number, $Ha = B_0 \sqrt{\frac{\sigma}{\rho E}}$ is the magnetic field parameter and $Pr Re = \frac{\rho C_P E a^2}{\kappa}$ is the product of the Prandtl number and the Reynolds number (i.e. Peclet number).

The similarity form of solution (Berman, 1953) is below.

$$\bar{\Psi} = \bar{z} F(\bar{r}), \quad \bar{\omega} = -\bar{z} G(\bar{r}), \quad \bar{T} = \theta(\bar{r}) \quad (2.14)$$

Equations (2.8), (2.12), (2.13) and (2.14) become

$$G = \frac{d}{d\bar{r}} \left[\frac{1}{\bar{r}} \frac{dF}{d\bar{r}} \right] \quad (2.15)$$

$$\frac{d}{d\bar{r}} \left[\frac{1}{\bar{r}} \frac{d(\bar{r}G)}{d\bar{r}} \right] = Re \left[\frac{G}{\bar{r}} \frac{dF}{d\bar{r}} - F \frac{d}{d\bar{r}} \left(\frac{G}{\bar{r}} \right) - Ha^2 G \right] \quad (2.16)$$

$$\frac{d}{d\bar{r}} \left[\bar{r} \frac{d\theta}{d\bar{r}} \right] = Pr Re \left[\theta \frac{dF}{d\bar{r}} - F \frac{d\theta}{d\bar{r}} \right] \quad (2.17)$$

The boundary conditions (2.5) and (2.6) become

$$F = 0, \quad \frac{d}{d\bar{r}} \left(\frac{1}{\bar{r}} \frac{dF}{d\bar{r}} \right) = 0, \quad \frac{d\theta}{d\bar{r}} = 0 \quad \text{on } \bar{r} = 0 \quad (2.18)$$

$$F = -1, \quad \frac{dF}{d\bar{r}} = 1, \theta = 1 \quad \text{on } \bar{r} = 1 \quad (2.19)$$

For small Re we seek the solution of the equations (2.15)-(2.17) as a perturbation series in terms of the parameter Re i.e.

$$\omega(\bar{r}) = \sum_{i=0}^n \omega_i Re^i \quad (2.20)$$

$$\theta(\bar{r}) = \sum_{i=0}^n \theta_i Re^i \quad (2.21)$$

Where ω can be either $F(\bar{r}, Re)$ or $G(\bar{r}, Re)$.

Substituting equations (2.20) and (2.21) into equations (2.16)-(2.19), neglecting the bars for clarity, and collecting the coefficients of like powers of Re , the resulting equations are

$$G_n = \left[\frac{1}{r} F'_n \right]' \quad (2.22)$$

$$\left[\frac{1}{r} (rG_n)' \right]' = Re \sum_{i=0}^{n-1} \left[G_i \left(\frac{F'_{n-i-1}}{r} \right) - F_i \left(\frac{G'_{n-i-1}}{r} \right) - Ha^2 G_i \right] \quad (2.23)$$

$$[r\theta'_n]' = Pr Re \sum_{i=0}^{n-1} [\theta_i F'_{n-i-1} - F_i \theta'_{n-i-1}] \quad (2.24)$$

$$F_n = 0, \quad \left[\frac{1}{r} F'_n \right]' = 0, \quad \theta'_n = 0 \quad \text{on } r = 0 \quad (2.25)$$

$$F_0 = -1, \quad F_{n+1} = 0, \quad F'_0 = 1, \quad F'_{n+1} = 0 \quad \theta_n = 1 \quad \text{on } r = 1 \quad (2.26)$$

Where $n = 0, 1, 2, \dots$ and the prime symbol denotes differentiation with respect to r . Solving equations (2.23) and (2.24) using (2.26) and (2.27), we obtain the first 52 terms of F and G . Here we represent some of them.

$$F_0 = \frac{1}{2}r^2(3r^2 - 5)$$

$$F_1 = \left(-\frac{3}{16} - \frac{1}{16}Ha^2\right)r^2 + \left(\frac{7}{16} + \frac{1}{8}Ha^2\right)r^4 + \left(-\frac{5}{16} - \frac{1}{16}Ha^2\right)r^6 + \frac{1}{16}r^8 \quad (2.27)$$

$$G_0 = 12r$$

$$G_1 = \left(\frac{7}{2} + Ha^2\right)r + \left(-\frac{15}{2} - \frac{3}{2}Ha^2\right)r^3 + 3r^5 \quad (2.28)$$

The stream function $F(r)$ and shear stress $G(r)$ is represented as

$$F(r) = \frac{1}{2}r^2(3r^2 - 5) + \left(\left(-\frac{3}{16} - \frac{1}{16}Ha^2\right)r^2 + \left(\frac{7}{16} + \frac{1}{8}Ha^2\right)r^4 + \left(-\frac{5}{16} - \frac{1}{16}Ha^2\right)r^6 + \frac{1}{16}r^8\right)Re + O(Re^2) \quad (2.29)$$

$$G(r) = 12r + \left(\left(\frac{7}{2} + Ha^2\right)r + \left(-\frac{15}{2} - \frac{3}{2}Ha^2\right)r^3 + 3r^5\right)Re + O(Re^2) \quad (2.30)$$

Solving (2.25) using (2.26), (2.27) and (2.28), we obtain the first two terms of θ as

$$\theta_0 = 1$$

$$\theta_1 = 1 + \frac{7}{8}PrRe - \frac{5}{4}PrRe r^2 + \frac{3}{8}PrRe r^4 \quad (2.31)$$

Substituting (2.32) into (2.22), we have

$$\theta = 1 + \left(1 + \frac{7}{8}PrRe - \frac{5}{4}PrRe r^2 + \frac{3}{8}PrRe r^4\right)Re + O(Re^2) \quad (2.32)$$

Hence $T = z \theta(r)$ becomes

$$T = z \left(1 + \left(1 + \frac{7}{8} Pr Re - \frac{5}{4} Pr Re r^2 + \frac{3}{8} Pr Re r^4 \right) Re + O(Re^2) \right) \quad (2.33)$$

Equation (2.33) represents the temperature distribution of the fluid flow pattern in the tube.

The wall shear stress $G(1)$ is given by

$$G(1) = 12 + \left(-1 - \frac{17}{105} Ha^2 \right) Re + \left(-\frac{11}{30} - \frac{689}{10395} Ha^2 + \frac{229}{2646000} Ha^4 \right) Re^2 \dots \dots \dots \quad (2.34)$$

Also the rate of heat transfer across the wall $Nu = -\frac{d\theta}{dr}$ on $r = 1$ is given as

$$Nu = Pr Re + \left(-Pr - \frac{19}{16} Pr^2 \right) Re^2 - \left(-Pr - \frac{119}{96} Pr^2 - \frac{767}{83160} Pr^2 Ha^2 - \frac{73}{64} Pr^3 \right) Re^3 \dots \quad (2.35)$$

Shear stress consists of Reynolds number and Magnetic field parameter. On the other hand, the rate of heat transfer is controlled by the Prandtl number, Reynolds number and Magnetic field parameter.

2.3 COMPARISON OF SERIES SOLUTION

Many researchers demonstrate their interest on wall driven flow. We mainly observed and reproduced all the graphs of the paper of Makinde et al. (2006) using our series where they described the wall driven incompressible viscous flow through a tube and focused the effect of Prandtl number and Reynolds number on temperature, rate of heat transfer and shear stress are displayed below.

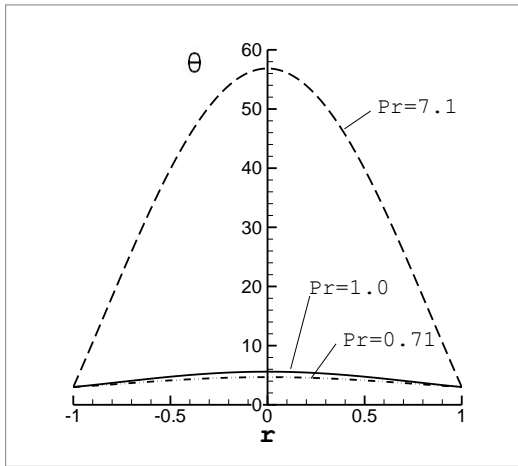


Figure 2.1: Temperature distribution ($Re=1$)

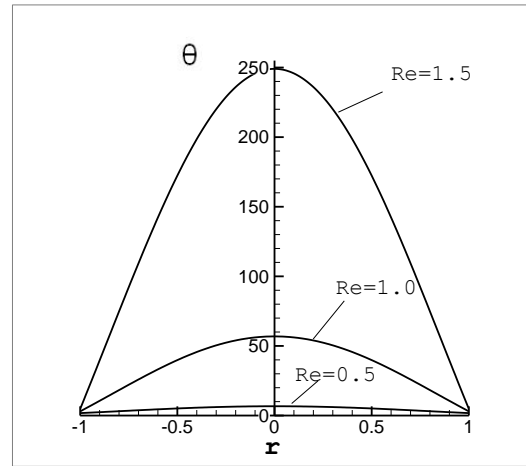


Figure 2.2: Temperature distribution ($Pr=7.1$)

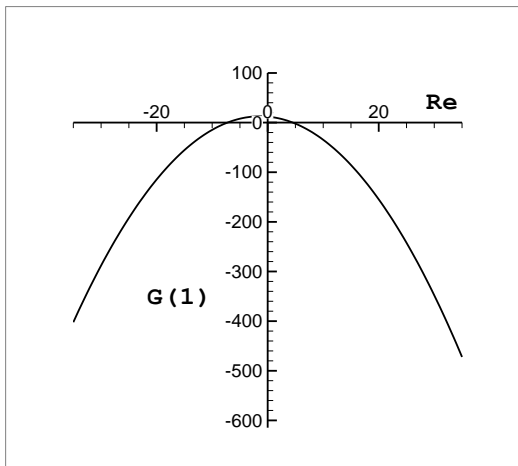


Figure 2.3: The wall shear stress versus Reynolds number

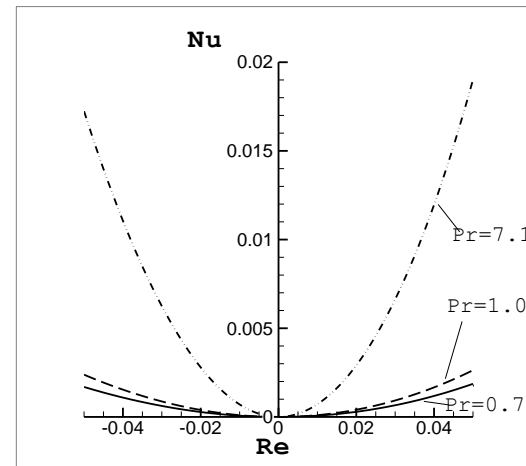


Figure 2.4: Heat transfer versus Reynolds number

Temperature increases with increase of Prandtl number and Reynolds number. Shear stress is parabolic in nature with maximum shear stress of $G(1) = 12$ corresponding to $Re = 0$. The rate of heat transfer increases with increase of Reynolds number and Prandtl number.

2.4 RESULT AND DISCUSSION

In this chapter, our main concern is to focus the effect of magnetic field on the wall driven flow through a tube. Here we discuss the magnetic effect on critical Reynolds number, velocity, temperature and rate of heat transfer.

2.4.1 Stability Analysis

Stability analysis is a very important measure of fluid dynamics. In this topic, stability of flow depends on Reynolds number as well as magnetic field parameter. The magnetic effect on critical Reynolds number is investigated using Drazin and Tourigny (1996) method.

The table below describes the critical value of Reynolds number and critical exponent of the series for different degree of approximation method.

Table 2.1: Critical Reynolds number and convergence of series

d	N	Re_c	α_c
2	7	1.896440685191754385393533376278298109137	0.14309372552923471272
3	12	1.855555297011919084542066622465085810909	0.5011432705264477896
4	18	1.855615791833465515448011802910196755818	0.5000654158029171952
5	25	1.855617095905333898765805967710516717693	0.500000401206471702
6	33	1.855617096301163238736762524848150427362	0.500000000055305208
7	42	1.855617096301194304949411235916147573222	0.500000000000006897
8	52	1.855617096301194307370092402753737201182	0.500000000000000017

Here, d indicates the degree or order of the approximation method, N represents the number of terms is used in approximation method, Re_c represents the critical Reynolds number for stability, α_c is the critical exponent that indicates convergence of the series.

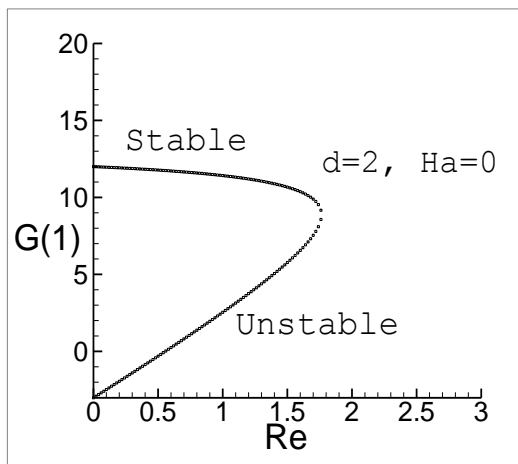


Figure 2.5 (a): Shear stress versus Reynolds number

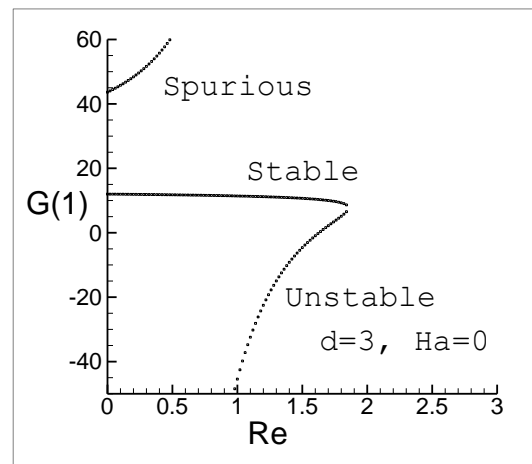


Figure 2.5 (b): Shear stress versus Reynolds number

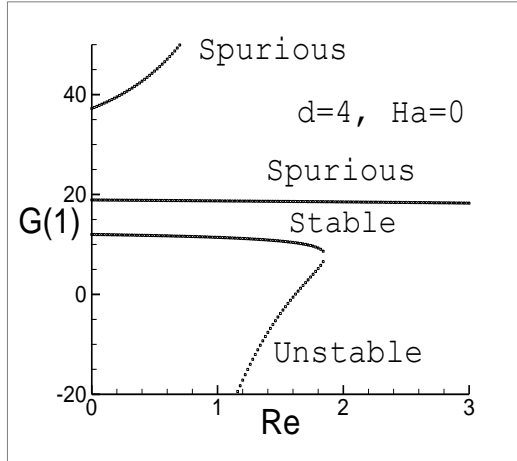


Figure 2.5 (c): Shear stress versus Reynolds number

Figures 2.5 (a,b,c) represent the shear stress versus Reynolds number. These figures are drawn according to the approximation of Drazin and Tourigny (1996). Generally, this enables us to obtain solution branches of the series problem. These figures indicate the critical Reynolds number (maximum Reynolds number for laminar flow) is 1.855. Flow within this critical Reynolds number is laminar and the beyond this Reynolds number is turbulent.

It is very clear from this table that the increase of Magnetic effect decreases the critical Reynolds number and increase the scope of instability.

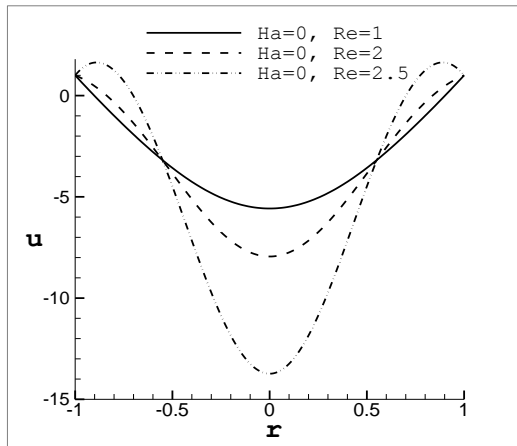


Figure (2.6) : Velocity versus distance from center for different Reynolds number.

Figure (2.6) demonstrates the curve of velocity versus distance from center of the tube on different Reynolds number. the Reynolds number for the solid curve is one (within critical Reynolds number) where the velocity profile is parabolic and flow is laminar. The Reynolds number of other two curves is higher than the critical limit where velocity profile change its shape become chaotic and the flow is unstable.

2.4.2 Hydro magnetic Effect

In this section, we demonstrate the effect of magnetic field on critical Reynolds number, velocity, temperature and rate of heat transfer.

The table below describes critical Reynolds number and critical exponent for different Hartmann number.

Table 2.2: Magnetic effect on the critical Reynolds number

Ha	Re_c	α_c
0	1.855617096301194307370092402753737201182	0.50000000000000000017
1	1.638108201874584719607741425559563592311	0.50000000000000000011
2	1.239888494401073609369135616633954544803	0.50000000000000000015
3	0.9077797498781283388121675356039423477681	0.49999999999999999987
4	0.6743496105532700649617455094493058845383	0.50000000000000000071
5	0.5140860675518937643664582692218663298302	0.50000000000000000098
6	0.4022324127049437013339760901700789123709	0.499999999999999999879
7	0.3221079026305581527128502997992374818216	0.499999999999999999883
8	0.2631670688144713895249751751246670407251	0.50000000000000019006
15	0.09257273145910536963336024511472910148543	0.50000000000000032051
20	0.05529930523597997025023808856228618046559	0.500000000000000395214

Here, increase of Hartmann number decreases the critical Reynolds number and enhances the scope of instability.

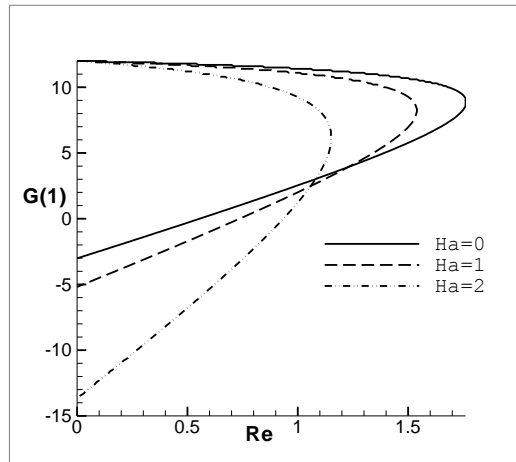


Figure (2.7) : Shear stress versus Reynolds number for different Magnetic field values.

Figure (2.7) illustrates the Shear stress versus Reynolds number on different magnetic field parameter. This figure is drawn according to the approximation of Drazin and Tourigny (1996). These figures describe the critical Reynolds number is shift towards the origin with the increases of Magnetic field parameter (Hydro magnetic effect). Increase of magnetic effect decreases the critical Reynolds number and enhances the scope of instability. Physically, magnetic field creates an opposite velocity along the tube that distorts the main flow.

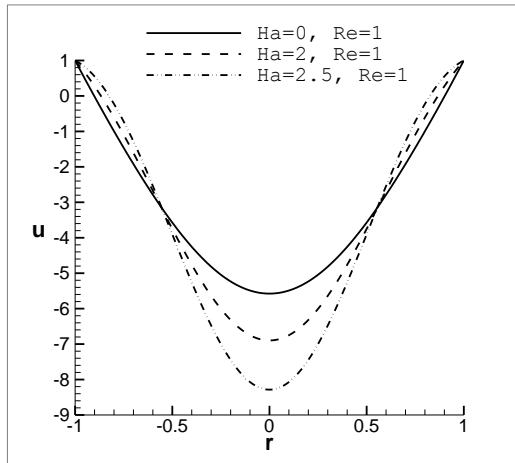


Figure (2.8) : Velocity versus distance from center for different Magnetic field values.

Figure (2.8) illustrates the velocity versus distance from center for different magnetic field parameter. Velocity is induced by the wall driven force so the velocity of fluid at the wall is one. At the center of the tube, velocity is negative where flow is in the opposite direction. Magnetic effect creates a negative force along the flow so increase of magnetic field parameter increases the negative velocity (decreases the velocity) at the center of the tube.

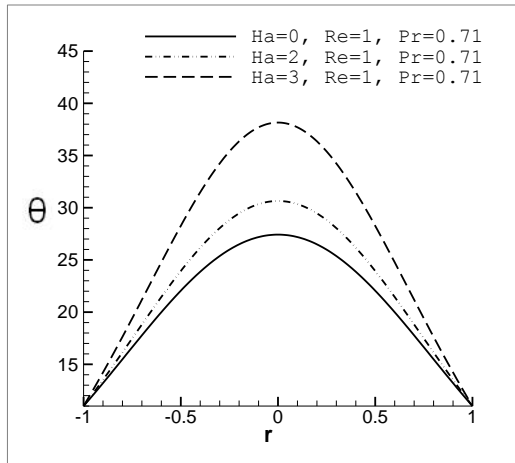


Figure (2.9) : Temperature versus distance from center for different Magnetic field values

Figure (2.9) illustrates the temperature versus the distance from center for different value of magnetic field parameter. The increase of magnetic field intensity increases opposite force that creates thermal conduction from heated wall. So, increase of magnetic field intensity increases the temperature of the center of the tube.

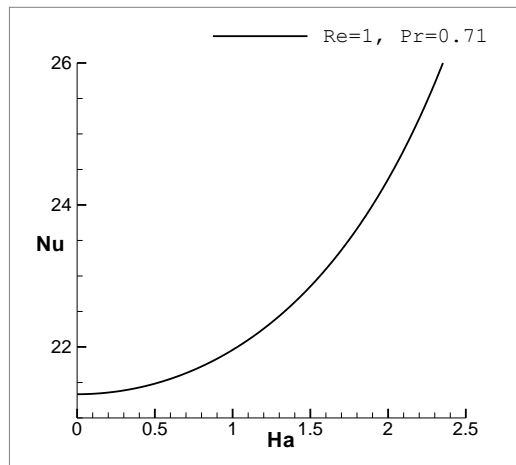


Figure (2.10) : Nusselt number versus Magnetic field intensity.

Figure (2.10) demonstrates the Nusselt number versus Magnetic field parameter. Magnetic effect creates an opposite flow towards the main flow. This opposite flow increases temperature due to thermal conduction from heated wall. So, magnetic field parameter increases the temperature of the fluid. That is why, the rate of heat transfer increases with increases of Magnetic field parameter.

2.5 CONCLUSION

Magnetic effect on fluid flow and heat transfer through a porous tube is very significant. In this chapter, the hydro-magnetic effect on critical Reynolds number, velocity, temperature and rate of heat transfer are analyzed. The result reveals the followings.

- 1) Magnetic effect decreases the magnitude of critical Reynolds number which increases the scope of instability.
- 2) Magnetic effect decreases the velocity and increases the temperature of the fluid.
- 3) Magnetic effect enhances the rate of heat transfer.

Chapter 3

MHD effect on fluid flow and heat transfer through a collapsible tube

3.1 INTRODUCTION

In human body, all the conduits are flexible and collapsible. That is, when the external pressure exceeds the internal pressure, the tube cross-sectional area can be significantly reduced, but not fully diminished. Many researchers worked on collapsible tube due to its extensive use in human body and different sophisticated machineries. Contrad (1969), Cowley (1982, 1983), Heil (1997), Makinde et al. (2002) have comprehensive contribution on elastic or collapsible tube. Specially, Makinde (2005) represented the perturbation technique to solve the collapsible tube problem. He also performed the bifurcation study with a special type of Hermite-Padé approximants.

In this chapter, a mathematical model describing the fluid dynamics of a collapsible tube with thermal and magnetic effect is presented. Analytical solutions are constructed for the problem using approximation technique. The computer extension of the resulting power series solutions, its analysis and analytic continuation is performed.

3.2. PHYSICAL MODEL

The problem under consideration is that of unsteady flow of a viscous incompressible fluid in a collapsible tube. Take a cylindrical coordinate system (r, z) where oz lies along the centre of the tube, r is the distance measured radially. Let u and v be the velocity components in the directions of length and radius of the tube respectively. It is assumed that the tube's wall is at $r = a_0$ (characteristic radius of the tube) at time $t = 0$ as shown in figure below.

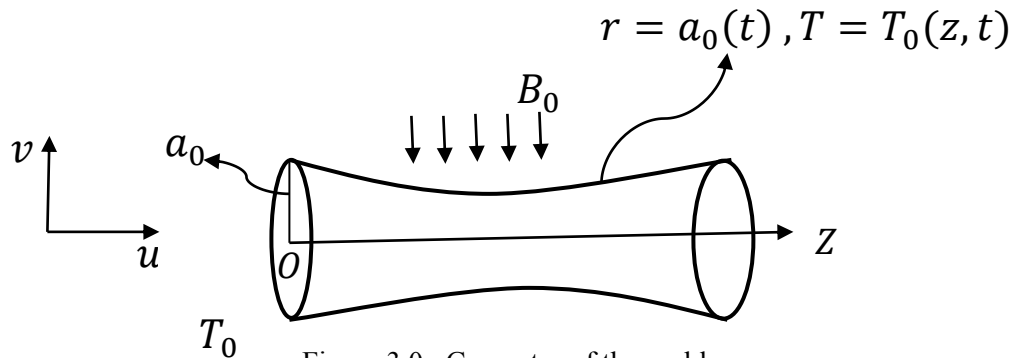


Figure 3.0: Geometry of the problem

Then, for axisymmetric unsteady viscous incompressible flow, the continuity, Navier-Stokes, Energy equations are

The equation of continuity is

$$\frac{\partial}{\partial r}(rv) + r \frac{\partial u}{\partial z} = 0 \quad (3.1)$$

the Navier-Stokes equations

$$\frac{\partial u}{\partial t} + u \frac{\partial u}{\partial z} + v \frac{\partial u}{\partial r} = -\frac{1}{\rho} \frac{\partial P}{\partial z} + \nu \nabla^2 u - B_0^2 \frac{\sigma}{\rho} u \quad (3.2)$$

$$\frac{\partial v}{\partial t} + u \frac{\partial v}{\partial z} + v \frac{\partial v}{\partial r} = -\frac{1}{\rho} \frac{\partial P}{\partial r} + \nu \left(\nabla^2 v - \frac{v}{r^2} \right) \quad (3.3)$$

Energy equation

$$\rho C_p \left\{ \frac{\partial T}{\partial t} + u \frac{\partial T}{\partial z} + v \frac{\partial T}{\partial r} \right\} = \kappa \nabla^2 T \quad (3.4)$$

Where $\nabla^2 = \frac{\partial^2}{\partial r^2} + \frac{\partial}{r \partial r} + \frac{\partial^2}{\partial z^2}$, P is the pressure, ρ the density and ν the kinematic viscosity of the fluid, T is the temperature, κ the coefficient of thermal conductivity, μ the coefficient of viscosity and C_p is the specific heat capacity at constant pressure.

The appropriate boundary conditions are:

Along z-axis

$$\frac{\partial u}{\partial r} = 0, v = 0, \quad \frac{\partial T}{\partial r} = 0 \quad \text{on } r = 0 \quad (3.5)$$

The axial and normal velocities at the wall are prescribed as

$$u = 0, \quad v = \frac{da}{dt}, \quad T = \frac{T_0 z}{a_0 \sqrt{1 - at}} \quad \text{on } r = a(t) \quad (3.6)$$

We introduce the stream-function Ψ , vortices ω is the following manner:

$$u = \frac{1}{r} \frac{\partial \psi}{\partial r} \quad \text{and} \quad v = -\frac{1}{r} \frac{\partial \psi}{\partial z} \quad (3.7)$$

$$\omega = \frac{\partial v}{\partial z} - \frac{\partial u}{\partial r} = -\frac{1}{r} \frac{\partial^2 \psi}{\partial z^2} - \frac{1}{r} \frac{\partial^2 \psi}{\partial r^2} + \frac{1}{r^2} \frac{\partial \psi}{\partial r} \quad (3.8)$$

Eliminating pressure P from (3.2), (3.3), (3.4),(3.5) and (3.6) by using (3.7) and (3.8) we get:

$$\frac{\partial \omega}{\partial t} + \frac{1}{r} \frac{\partial(\psi, \omega)}{\partial(r, z)} + \frac{\omega}{r^2} \frac{\partial \psi}{\partial z} - B_0^2 \frac{\sigma}{\rho} \frac{\partial}{\partial r} \left(\frac{1}{r} \frac{\partial \Psi}{\partial r} \right) = \nu \left[\nabla^2 \omega - \frac{\omega}{r^2} \right], \quad \omega = -\nabla^2 \psi \quad (3.9)$$

$$\frac{\partial T}{\partial t} + \frac{1}{r} \frac{\partial(\psi, T)}{\partial(r, z)} = \frac{\kappa}{\rho C_p} \nabla^2 T \quad (3.10)$$

$$\frac{\partial \psi}{\partial r} = 0, \quad \frac{\partial \psi}{\partial z} = -a \frac{da}{dt}, \quad T = \frac{T_0 z}{a_0 \sqrt{1 - \alpha t}} \quad \text{on} \quad r = a(t) \quad (3.11)$$

$$\frac{\partial}{\partial r} \left(\frac{1}{r} \frac{\partial \psi}{\partial r} \right) = 0, \quad \frac{\partial \psi}{\partial z} = 0, \quad \frac{\partial T}{\partial r} = 0 \quad \text{on} \quad r = 0 \quad (3.12)$$

We introduce the following transformations:

$$\eta = \frac{r}{a_0 \sqrt{1 - \alpha t}}, \quad \Psi = \frac{\alpha z F(\eta) a_0^2}{2}, \quad \omega = \frac{\alpha z G(\eta)}{2 a_0 (\sqrt{1 - \alpha t})^3}, \quad T = \frac{T_0 z \theta(\eta)}{a_0 \sqrt{1 - \alpha t}} \quad (3.13)$$

Substituting equation (3.13) into equations (3.9) – (3.12), we obtain;

$$\frac{d}{d\eta} \left[\frac{1}{\eta} \frac{d(\eta G)}{d\eta} \right] = Re \left[\frac{G}{\eta} \frac{dF}{d\eta} - F \frac{d}{d\eta} \left(\frac{G}{\eta} \right) + \eta \frac{dG}{d\eta} + 3G + Ha^2 G \right], \quad G = -\frac{d}{d\eta} \left(\frac{1}{\eta} \frac{dF}{d\eta} \right) \quad (3.14)$$

$$\frac{d}{d\eta} \left(\eta \frac{d\theta}{d\eta} \right) = Pr Re \left[\theta \frac{dF}{d\eta} - F \frac{d\theta}{d\eta} + \eta^2 \frac{d\theta}{d\eta} + \eta \theta \right] \quad (3.15)$$

$$\frac{dF}{d\eta} = 0, \quad F = 1, \quad \theta = 1 \quad \text{on} \quad \eta = 1 \quad (3.16)$$

$$\frac{d}{d\eta} \left(\frac{1}{\eta} \frac{dF}{d\eta} \right) = 0, \quad F = 0, \quad \frac{d\theta}{d\eta} = 0 \quad \text{on} \quad \eta = 0 \quad (3.17)$$

Where $Re = a_0^2 \alpha / 2\nu$ is the local Reynolds number ($Re > 0$ represents contraction while $Re < 0$ represents expansion of the tube's wall). $RePr = \frac{\rho C_p a_0^2}{2K} \alpha$, $Ha = B_0 \sqrt{\frac{2\sigma}{\rho\alpha}} (1 - \alpha t)$ is the magnetic field parameter.

Method of solution

To solve equations (3.14)-(3.17), it is convenient to take a power series expansion in terms of local Reynolds number Re ie.

$$F = \sum_{i=0}^n F_i Re^i, \quad G = \sum_{i=0}^n G_i Re^i, \quad \theta = \sum_{i=0}^n \theta_i Re^i \quad (3.18)$$

Substitute (3.18) into equations (3.14)-(3.17) and collecting the coefficients of like power of Re , we obtain the following :

Zerth Order:

$$\frac{d}{d\eta} \left(\frac{1}{\eta} \frac{d(\eta G_0)}{d\eta} \right) = 0, \quad G_0 = -\frac{d}{d\eta} \left(\frac{1}{\eta} \frac{dF_0}{d\eta} \right) \quad \frac{d}{d\eta} \left(\eta \frac{d(\theta_0)}{d\eta} \right) = 0 \quad (3.19)$$

$$\frac{dF_0}{d\eta} = 0, \quad F_0 = 1, \quad \theta_0 = 1 \quad \text{on} \quad \eta = 1 \quad (3.20)$$

$$\frac{d}{d\eta} \left(\frac{1}{\eta} \frac{dF_0}{d\eta} \right) = 0, \quad F_0 = 0, \quad \frac{d\theta_n}{d\eta} = 0 \quad \text{on} \quad \eta = 0 \quad (3.21)$$

Higher Order ($n \geq 1$):

$$\frac{d}{d\eta} \left(\frac{1}{\eta} \frac{d(\eta G_n)}{d\eta} \right) = Re \left[\sum_{i=0}^{n-1} \left(\frac{G_i}{\eta} \frac{dF_{n-i+1}}{d\eta} - F_i \frac{d}{d\eta} \left(\frac{G_{n-i-1}}{\eta} \right) \right) + \eta \frac{dG_{n-1}}{d\eta} + 3G_{n-1} + Ha^2 G_{n-1} \right],$$

$$G_n = \frac{d}{d\eta} \left(\frac{1}{\eta} \frac{dF_n}{d\eta} \right), \quad (3.22)$$

$$\frac{d}{d\eta} \left(\eta \frac{d\theta_n}{d\eta} \right) = Pr \left[\sum_{i=0}^{n-1} \left(\theta_i \frac{dF_{n-i-1}}{d\eta} - F_i \frac{d\theta_{n-i-1}}{d\eta} \right) + \eta^2 \frac{d\theta_{n-1}}{d\eta} + \eta \theta_{n-1} \right]$$

$$\frac{dF_n}{d\eta} = 0, \quad F_n = 0, \quad \theta_n = 0 \quad \text{on} \quad \eta = 1 \quad (3.23)$$

$$\frac{d}{d\eta} \left(\frac{1}{\eta} \frac{dF_n}{d\eta} \right) = 0, \quad F_n = 0, \quad \frac{d\theta_n}{d\eta} = 0 \quad \text{on} \quad \eta = 0 \quad (3.24)$$

We have written a MAPLE program that calculates successively the coefficients of the solution series.

$$\begin{aligned}
F(\eta) = & 2\eta^2 - \eta^4 + \left(\left(-\frac{5}{18} - \frac{1}{24}Ha^2 \right) \eta^2 + \left(\frac{7}{12} + \frac{1}{12}Ha^2 \right) \eta^4 + \left(-\frac{1}{24}Ha^2 - \frac{1}{3} \right) \eta^6 + \frac{1}{36} \eta^8 \right) Re \\
& + \left(\left(\frac{1}{576}Ha^4 + \frac{1057}{10800} + \frac{113}{4320}Ha^2 \right) \eta^2 + \left(-\frac{271}{1080} - \frac{191}{2880}Ha^2 - \frac{5}{1152}Ha^4 \right) \eta^4 \right. \\
& + \left(\frac{47}{216} + \frac{1}{18}Ha^2 + \frac{1}{288}Ha^4 \right) \eta^6 + \left(-\frac{2}{27} - \frac{29}{1728}Ha^2 - \frac{1}{1152}Ha^4 \right) \eta^8 \\
& \left. + \left(\frac{7}{720} + \frac{1}{720}Ha^2 \right) \eta^{10} - \frac{1}{5400} \eta^{12} \right) Re^2 + O(Re^3)
\end{aligned} \tag{3.25}$$

$$\begin{aligned}
G(\eta) = & 8\eta + \left(\left(-\frac{14}{3} - \frac{2}{3}Ha^2 \right) \eta + (Ha^2 + 8)\eta^3 - \frac{4}{3}\eta^5 \right) Re \\
& + \left(\left(\frac{271}{135} + \frac{191}{360}Ha^2 + \frac{5}{144}Ha^4 \right) \eta + \left(-\frac{47}{9} - \frac{4}{3}Ha^2 - \frac{1}{12}Ha^4 \right) \eta^3 \right. \\
& + \left(\frac{32}{9} + \frac{29}{36}Ha^2 + \frac{1}{24}Ha^4 \right) \eta^5 + \left(-\frac{7}{9} - \frac{1}{9}Ha^2 \right) \eta^7 + \frac{1}{45} \eta^9 \left. \right) Re^2 \\
& + O(Re^3)
\end{aligned} \tag{3.26}$$

$$\begin{aligned}
\theta(\eta) = & 1 + \left(-Pr + \frac{5}{4}Pr \eta^2 - \frac{1}{4}Pr \eta^4 \right) Re \\
& + \left(\frac{13}{288}Pr + \frac{485}{576}Pr^2 + \frac{1}{144}Pr Ha^2 + \left(-\frac{5}{4}Pr^2 - \frac{5}{36}Pr - \frac{1}{48}Pr Ha^2 \right) \eta^2 \right. \\
& + \left(\frac{31}{64}Pr^2 + \frac{7}{48}Pr + \frac{1}{48}Pr Ha^2 \right) \eta^4 \\
& + \left(-\frac{11}{144}Pr^2 - \frac{1}{144}Pr Ha^2 - \frac{1}{18}Pr \right) \eta^6 + \frac{1}{288}Pr \eta^8 \left. \right) Re^2 \\
& + O(Re^3)
\end{aligned} \tag{3.27}$$

The series of $F(\eta)$ represents the stream line which consists of Reynolds number and Magnetic field parameter. Similarly, the series $G(\eta)$ represents the shear stress that also consists of Reynolds number and Magnetic field parameter. However, the temperature is represented by the $\theta(\eta)$ which has three dimensionless number such as Reynolds number, Prandtl number and Hartmann number.

3.3 COMPARISON OF SERIES SOLUTION

Collapsible tube is a popular topic among the researcher. In this thesis, we observed and reproduced the graphs of the paper of Odejide et al. (2008) using our series where they described the laminar flow of an incompressible viscous fluid through a collapsible tube and focused on the effect of temperature along the tube as the increases of Reynolds number and Prandtl number. Those graphs are described below.

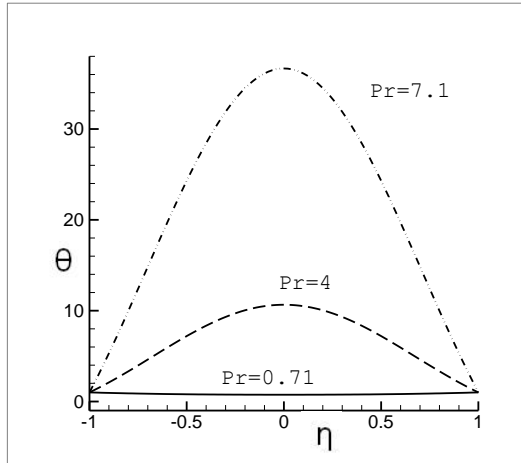


Figure 3.1: Temperature profile for different Prandtl number.

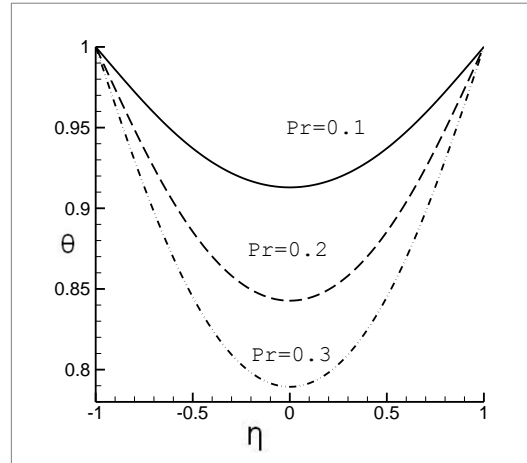


Figure 3.2: Temperature profile for different Prandtl number.

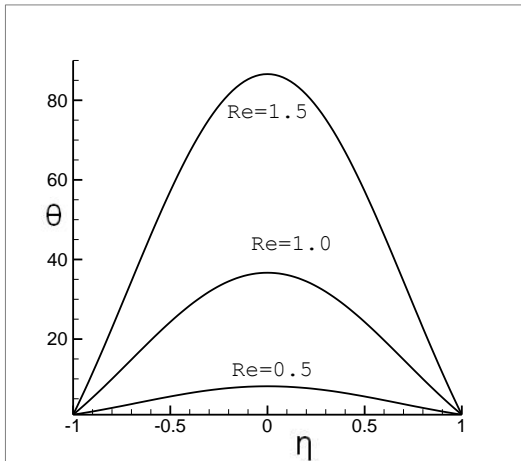


Figure 3.3: Temperature profile for different Reynolds number.

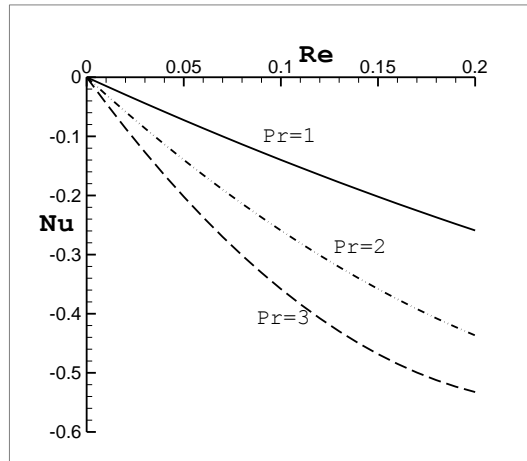


Figure 3.4: Nusselt number versus Reynolds number.

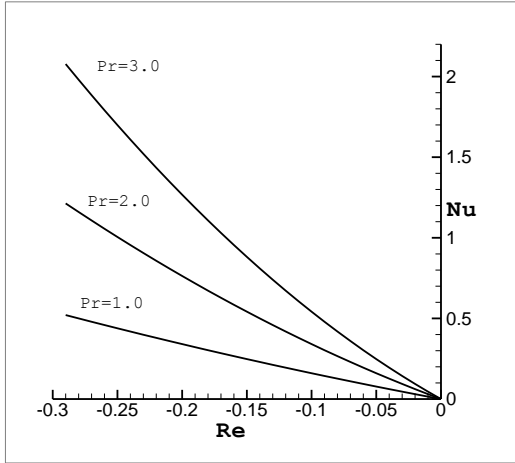


Figure 3.5: Nusselt number versus Reynolds number.

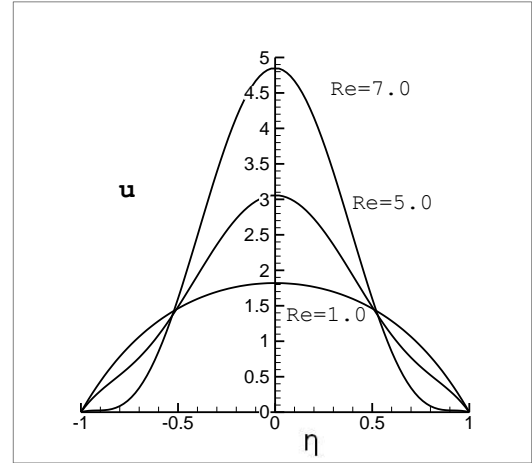


Figure 3.6: Velocity profile for different Reynolds number.

From the above graphs, it is very clear that temperature increases with increase of Reynolds number. Thermal behavior of the collapsible tube for the change of Prandtl number is dramatic. When the value of Prandtl number is less than one then temperature decreases with increases of Prandtl number. Whereas, the value of Prandtl number is greater than one then temperature increases with increases of Prandtl number. It is important to note that wall expansion is represented by negative values of flow Reynolds number ($Re < 0$) while wall contraction is represented by positive values of flow Reynolds number ($Re > 0$). The rate of heat transfer increases with increase of Prandtl number when the Reynolds number is negative. On the other hand, the rate of heat transfer decreases with the increase of Prandtl number when the Reynolds number is positive.

3.4 RESULT AND DISCUSSION

In this chapter, we focus on the effect of Magnetic field on collapsible tube. Here, we represent the magnetic effect on critical Reynolds number, velocity, temperature and rate of heat transfer.

3.4.1 Stability Analysis

Stability analysis is very significant issue for the fluid dynamics. Using approximation method (Drazin and Tourigny, 1996) the critical Reynolds number is determined.

The table below describes the critical value of Reynolds number and critical exponent of the series for different degree of approximation method.

Table 3.1: Critical Reynolds number and critical exponent

d	N	Re_c	α_c
2	7	-1.678295274145824762908903212789620190726	0.28855247649542405227
3	12	-1.674435369415888764713281828653548287784	0.4847843128226708516
4	18	-1.673938117622300488495796179886101039652	0.4999047587882879221
5	25	-1.673936734782069208912879201224538927240	0.4999999989355867503
6	33	-1.673936734772090594610251674277102045209	0.499999999980358454
7	42	-1.673936734772080863691199717732618868296	0.499999999999998898
8	52	-1.673936734772080863360033970733103868389	0.499999999999999995

Here, d indicates the degree or order of the approximation method, N represents the number of terms are used in approximation method, Re_c represents the critical Reynolds number for stability, α_c is the critical exponent that indicates convergence of the series.

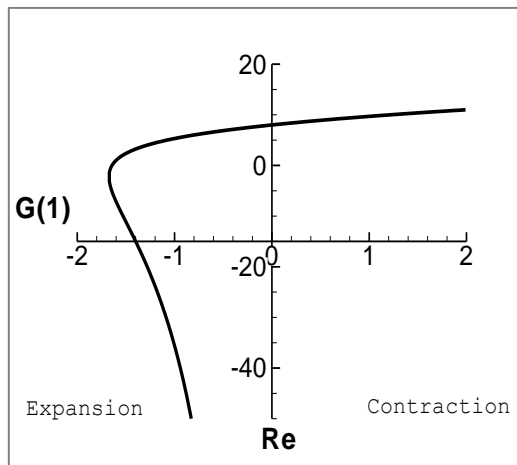


Figure 3.7: Shear stress versus Reynolds number

Figure (3.7) describes the shear stress versus Reynolds number. These figures are drawn according to approximation of Drazin and Tourigny (1996). Generally, this enables us to obtain solution branches of the series problem. These figures indicate the critical Reynolds number (maximum Reynolds number for laminar flow) is -1.6739. Reynolds number is always positive. The negative Reynolds number indicates the expansion of collapsible tube. So, the critical Reynolds number is 1.6739. Flow within this critical Reynolds number is stable and the beyond this Reynolds number is unstable.

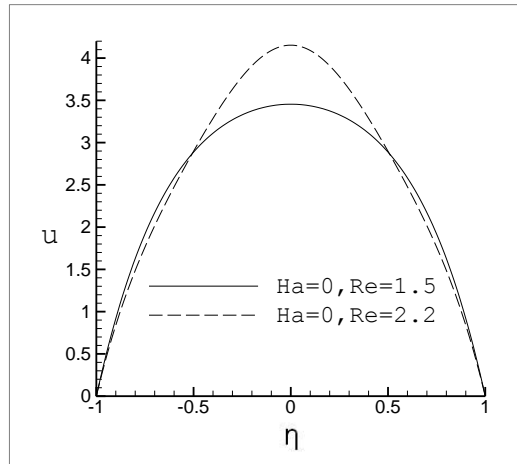


Figure 3.8: Velocity versus distance from center for different Reynolds number

Figure (3.8) demonstrates the curve of velocity versus distance from center on different Reynolds number. the reynolds number for the solid curve is 1.5 (within critical Reynolds number) where the velocity profile is parabolic and flow is laminar. the Reynolds number of other curve is 2.2 (higher than the critical limit) where velocity profile change its shape and the flow is unstable.

3.4.2 Effect of Magnetic Field on Critical Reynolds Number

In MHD flow, the effect of Hartmann number on stability and critical Reynolds number is very significant.

The table below describes critical Reynolds number and critical exponent for different Hartmann number.

Table 3.2: Magnetic effect on critical Reynolds number

Ha	Re_c	α_c
0	-1.673936734772080863691199717732618868296	0.499999999999998898
1	-1.527738503071394012401972021220987990984	0.499999999999998652
2	-1.219882420144165521295062416708963777195	0.4999999999999949670
3	-0.9247760150070194319014325730745220163455	0.4999999999999966897

Here, increase of Hartmann number decreases rapidly the critical Reynolds number and enhances the scope of instability.

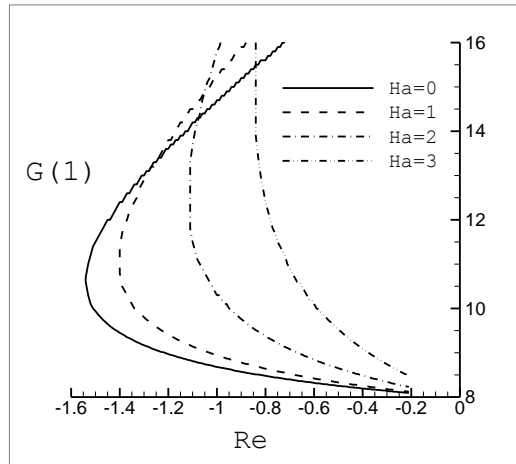


Figure 3.9: Shear stress versus Reynolds number for different Magnetic field values

Figure (3.9) illustrates the Shear stress versus Reynolds number on different Magnetic field parameter. This figure is drawn according to the approximation of Drazin and Tourigny (1996). These figures describe the critical Reynolds number is shift towards the origin with the increases of Magnetic field intensity (Hydro-magnetic effect). Increase of Magnetic field intensity decreases the critical Reynolds number and enhances the scope of instability.

3.4.3 Effect of Magnetic Field on Velocity and Temperature

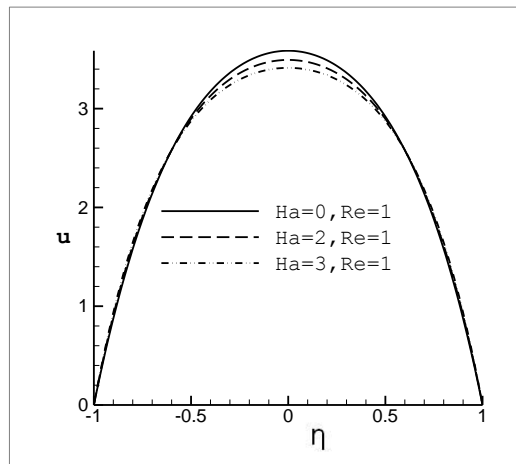


Figure 3.10: Velocity versus distance from center for different magnetic field parameter

The Figure (3.10) illustrates the cross sectional velocity profile for different magnetic field parameter. Magnetic field is applied along the tube that creates a force along the opposite direction of the flow that is why; increase of magnetic field parameter decreases the velocity.

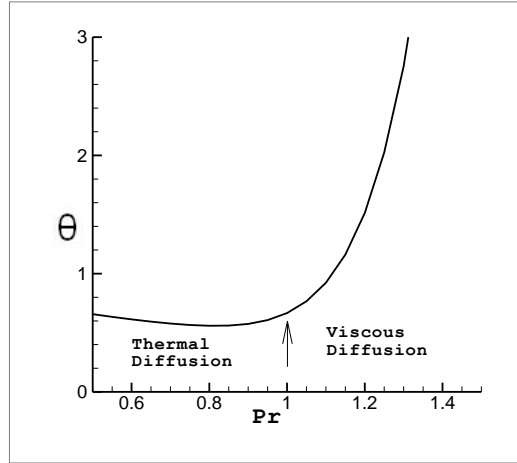


Figure 3.11: Temperature versus Prandtl number

The Figure (3.11) describes the temperature versus Prandtl number. Thermal behavior of fluid depends on the value of Prandtl number whether it is less than one or greater than one. When the value of Prandtl number is less than one, thermal diffusion is dominated where temperature slightly decreases with the increase of Prandtl number. However, the value of Prandtl number is greater than one, viscous diffusion is dominated that increases thermal convection and rises the temperature very rapidly.

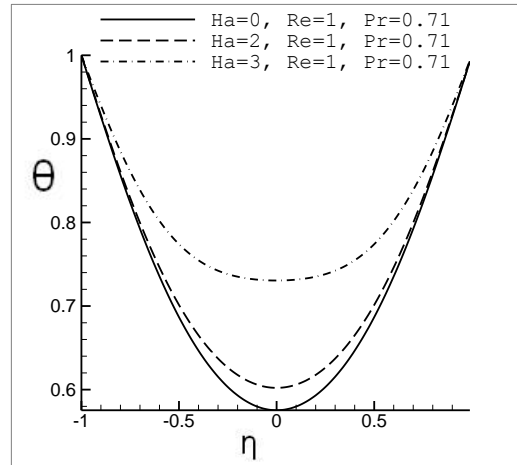


Figure 3.12: Temperature versus distance from center for different magnetic field parameter

Figure (3.12) describes the cross sectional temperature profile for different magnetic field parameter where maximum temperature at the wall and minimum temperature at the center of the tube. The value of Prandtl number (0.71) is less than one, thermal diffusion is occurred. Increase of Magnetic effect decreases the velocity that increases the thermal convection and rises the temperature.

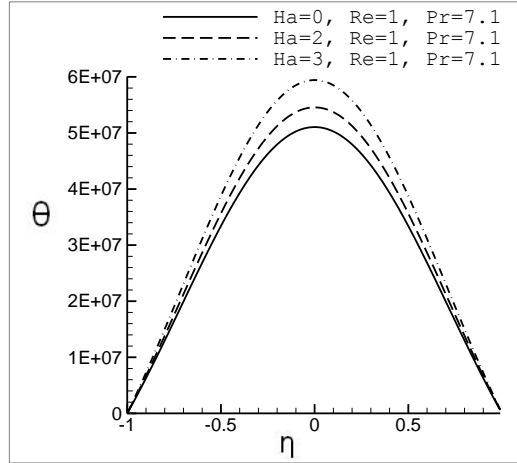


Figure 3.13: Temperature versus distance from center for different magnetic field parameter

Figure (3.13) illustrates the cross sectional temperature profile for different magnetic field parameter. This graph shows the maximum temperature at the center of the tube and minimum temperature at the wall. The value of Prandtl number is 7.1 where the viscous diffusion is occurred increase of magnetic effect decreases the velocity that increases the thermal convection and rises the temperature.

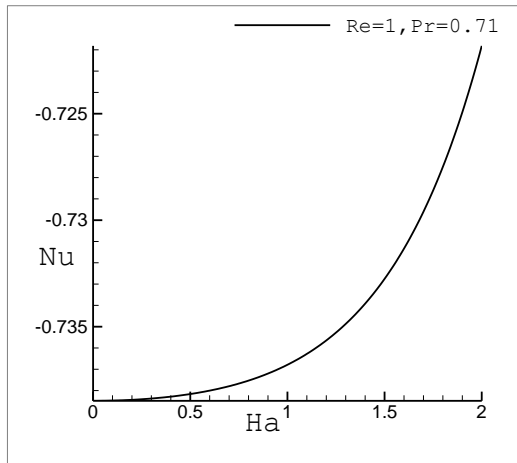


Figure 3.14: Nusselt number versus magnetic field parameter at Prandtl number < 1

The Figure (3.14) describes the Nusselt number versus magnetic field parameter on different Prandtl number. In figure (3.14), Prandtl number is less than one and wall temperature is higher than fluid. This figure displays the heat transfer from wall to the fluid that is why the rate of heat transfer is negative. Hartmann number increases the temperature due to thermal conduction at the center line of the tube that reduces the heat transfer rate.

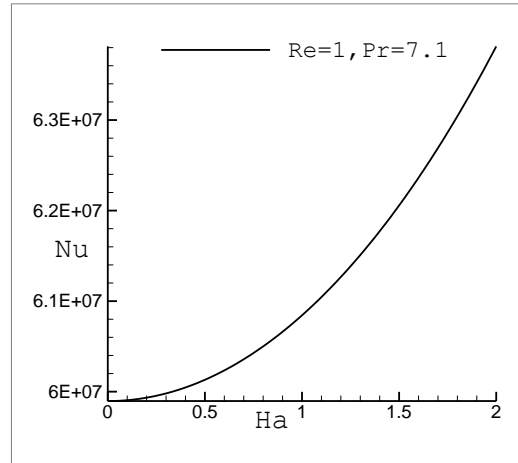


Figure 3.15: Nusselt number versus magnetic field parameter at Prandtl number > 1

The Figure (3.15) describes the Nusselt number versus magnetic field parameter on different Prandtl number. On the other hand, in figure (3.15), where Prandtl number greater than one and temperature at center is high than the temperature at wall. So the heat transfers from fluid to wall. Magnetic field creates a opposite flow that increase temperature due to thermal conduction from heated wall to fluid. High temperature at center increases the rate of heat transfer through wall.

3.5 CONCLUSION

Fluid flow through collapsible tube is very popular research topic. Many researchers investigate the behavior of collapsible tube due to its extensive use including human body. In this chapter, magnetic effect on collapsible is the main focused area. The findings of this study are described below.

- 1) Increase of magnetic effect decrease the value of critical Reynolds number that increases the scope of instability.
- 2) Increase of magnetic effect decreases the velocity of fluid.
- 3) Increase of magnetic effect increases the temperature and rate of heat transfer.

Chapter 4

MHD effect on fluid flow and heat transfer through a collapsible tube with obstacle and without obstacle

4.1 INTRODUCTION

Laminar flows in a tube or a collapsible tube with three-dimensional obstacles are common in nature and occur in many applications including oil industries, blood flow in veins, flow around tall buildings, bridges and vehicles. Understanding and predicting the properties of these flows are necessary for safe, effective and economical engineering designs. Experimental techniques are expensive and often provide data that is not sufficiently detailed. With the advent of computers it has become possible to investigate these flows using numerical simulations.

Numerous authors, for example Berman (1953), Norberg (1987), Mathelin et al. (2005), Makinde (2005) etc. have developed and generalized the exact solution for the flow in a pipe driven by uniform wall suction. The application of computer technologies and numerical methods for modeling the flow phenomena has been very popular due to their development which gives effective results. CFD programs (Computational Fluid Dynamics) permit an analysis of flow problems, at the same time rejecting the time consuming and costly research during the designing cycle or upgrading of devices. In case of research concerning flows in channels, numerical calculations give information which may be useful in hydraulics, aviation, chemical engineering and process engineering.

The results are presented in this chapter is to explain how the geometry of obstacles, contraction and expansion of tube affect the image of the flow and the formation of vortex structures. Numerical calculations for the flow problem were performed by solving equations describing a steady flow of fluid in a collapsible tube by using the finite element package. The finite element method (FEM) is one of the numerical methods that have received popularity due to its capability for solving complex problems. In this study FEM will be applied for discretization of the governing equations. It is assumed that the incoming fluid flows in the tube are two dimensional, viscous and incompressible. The solution of the governing equations along with the boundary conditions will be obtained through the Galerkin finite element formulation.

The remainder of this chapter is as follows. In section 4.2, the physical configurations of the current research interest are shown. Then the appropriate mathematical model (both governing equations and boundary conditions) is considered in section 4.3. Dimensional analysis of the mathematical model is presented in the section 4.4.

4.2 PHYSICAL MODEL

The geometry of the problem which is investigated in this chapter is depicted in fig. 4.0. A polar co-ordinate system is used with origin at the left middle point of the computational domain. The system consists of a collapsible tube of length L and radius a , wall of tube is collapsible where wall temperature T_w . The depth of contraction is d_c . Magnetic field B_0 is applied normal to the z axis. Another tube contains a solid adiabatic block as obstacle with diameter d_o . It is assumed that the incoming flow is at a uniform velocity U_0 and at the temperature T_0 .

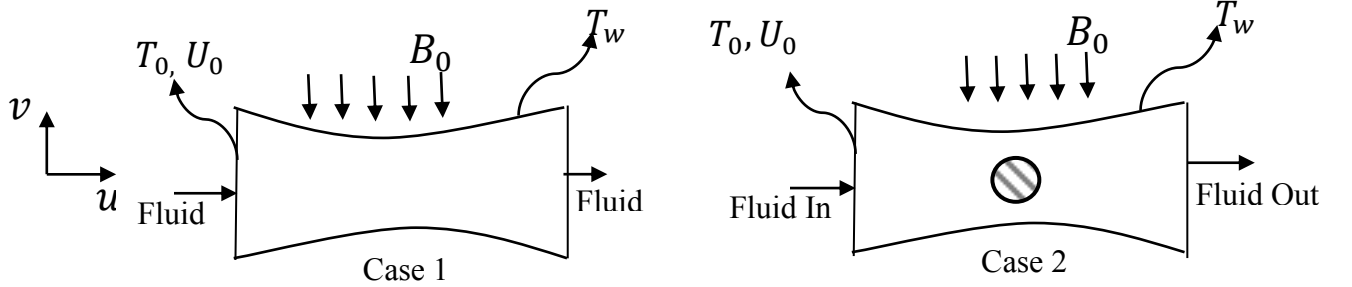


Figure 4.0: Geometry of Problem

4.3 GOVERNING EQUATION

The fundamental laws used to solve the fluid flow and heat transfer problems are the conservation of mass (continuity equations), conservation of momentums (momentum equations), and conservation of energy (energy equations), which constitute a set of coupled, nonlinear, partial differential equations. The governing equations for the two-dimensional flow expressed as

Continuity Equation

$$\frac{\partial rv}{\partial r} + r \frac{\partial u}{\partial z} = 0 \quad (4.1)$$

Momentum Equations

$$\frac{\partial u}{\partial t} + u \frac{\partial u}{\partial z} + v \frac{\partial u}{\partial r} = -\frac{1}{\rho} \frac{\partial P}{\partial z} + \nu (\nabla^2 u) - B_0^2 \frac{\sigma}{\rho} u \quad (4.2)$$

$$\frac{\partial v}{\partial t} + u \frac{\partial v}{\partial z} + v \frac{\partial v}{\partial r} = -\frac{1}{\rho} \frac{\partial P}{\partial r} + \nu \left(\nabla^2 v - \frac{v}{r^2} \right) \quad (4.3)$$

Energy Equation

$$\rho C_p \left(\frac{\partial T}{\partial t} + v \frac{\partial T}{\partial r} + u \frac{\partial T}{\partial z} \right) = \kappa \nabla^2 T \quad (4.4)$$

In this chapter, steady flow is considered. Then the governing equations become as below.

$$\frac{\partial rv}{\partial r} + r \frac{\partial u}{\partial z} = 0 \quad (4.5)$$

$$u \frac{\partial u}{\partial z} + v \frac{\partial u}{\partial r} = -\frac{1}{\rho} \frac{\partial P}{\partial z} + \nu (\nabla^2 u) - B_0^2 \frac{\sigma}{\rho} u \quad (4.6)$$

$$u \frac{\partial v}{\partial z} + v \frac{\partial v}{\partial r} = -\frac{1}{\rho} \frac{\partial P}{\partial r} + \nu \left(\nabla^2 v - \frac{v}{r^2} \right) \quad (4.7)$$

$$\rho C_p \left(v \frac{\partial T}{\partial r} + u \frac{\partial T}{\partial z} \right) = \kappa \nabla^2 T \quad (4.8)$$

Where r and z are the distance measured along the radius and horizontal directions respectively, u and v are the velocity components in the length and radius of the tube respectively, T and T_w denote the fluid and wall temperature respectively, T_0 denotes the initial temperature of the fluid, P is the pressure and ρ is the fluid density, C_p is the fluid specific heat, κ the thermal conductivity of fluid.

Boundary conditions

The boundary conditions for the present problem are specified as follows:

At the inlet

$$u = U_0, v = 0, T = T_0 \quad (4.9)$$

At the outlet

$$\frac{\partial u}{\partial z} = 0, v = 0, \frac{\partial T}{\partial z} = 0 \quad (4.10)$$

At the wall of the tube

$$u = 0, v = 0, T = T_w \quad (4.11)$$

4.4 DIMENSIONLESS ANALYSIS

Non-dimensional variables are used for making the governing equations (4.5-4.8) into dimensionless form are stated as follows:

$$\bar{r} = \frac{r}{a}, \quad \bar{z} = \frac{z}{a}, \quad \bar{u} = \frac{u}{U_0}, \quad \bar{v} = \frac{v}{U_0}, \quad \bar{P} = \frac{P}{\rho U_0^2}, \quad \theta = \frac{(T - T_w)}{(T_0 - T_w)} \quad (4.12)$$

Where \bar{z} and \bar{r} are the coordinates varying along horizontal and vertical directions respectively. \bar{u} and \bar{v} are the velocity components in the \bar{z} and \bar{r} directions respectively. θ is the dimensionless temperature and \bar{P} is the dimensionless pressure. After substitution of the dimensionless variables into the equations (4.5-4.8), we get the following dimensionless equations as.

$$\frac{\partial \bar{r} \bar{v}}{\partial \bar{r}} + \bar{r} \frac{\partial \bar{u}}{\partial \bar{z}} = 0 \quad (4.13)$$

$$\bar{u} \frac{\partial \bar{u}}{\partial \bar{z}} + \bar{v} \frac{\partial \bar{u}}{\partial \bar{r}} = -\frac{\partial \bar{P}}{\partial \bar{z}} + \frac{1}{Re} (\nabla^2 \bar{u}) - \frac{Ha^2}{Re} \bar{u} \quad (4.14)$$

$$\bar{u} \frac{\partial \bar{v}}{\partial \bar{z}} + \bar{v} \frac{\partial \bar{v}}{\partial \bar{r}} = -\frac{\partial \bar{P}}{\partial \bar{r}} + \frac{1}{Re} \left(\nabla^2 \bar{v} - \frac{\bar{v}}{\bar{r}^2} \right) \quad (4.15)$$

$$\left(\bar{v} \frac{\partial \theta}{\partial \bar{r}} + \bar{u} \frac{\partial \theta}{\partial \bar{z}} \right) = \frac{1}{Pr Re} \nabla^2 \theta \quad (4.16)$$

The dimensionless parameters appearing in the equations (4.13) to (4.16) are the Reynolds number Re , Prandtl number Pr , Hartmann number Ha , and solid fluid thermal conductivity ratio κ they are respectively defined as follows:

$$Re = \frac{U_0 a}{\nu}, \quad Pr = \frac{\nu \rho C_p}{\kappa}, \quad Ha = B_0 a \sqrt{\frac{\sigma}{\mu}} \quad (4.17)$$

The dimensionless boundary conditions under consideration can be written as:

At the inlet:

$$\bar{u} = 1, \quad \bar{v} = 0, \quad \theta = 1 \quad (4.18)$$

At the outlet:

$$\frac{\partial \bar{u}}{\partial \bar{z}} = 0, \quad \bar{v} = 0, \quad \frac{\partial \theta}{\partial \bar{z}} = 0 \quad (4.19)$$

At the wall of the tube

$$\bar{u} = 0, \quad \bar{v} = 0, \quad \theta = 0 \quad (4.20)$$

Eliminating bar sign, we get

$$\frac{\partial rv}{\partial r} + r \frac{\partial u}{\partial z} = 0 \quad (4.21)$$

$$u \frac{\partial u}{\partial z} + v \frac{\partial u}{\partial r} = -\frac{\partial P}{\partial z} + \frac{1}{Re} (\nabla^2 u) - \frac{Ha^2}{Re} u \quad (4.22)$$

$$u \frac{\partial v}{\partial z} + v \frac{\partial v}{\partial r} = -\frac{\partial P}{\partial r} + \frac{1}{Re} \left(\nabla^2 v - \frac{v}{r^2} \right) \quad (4.23)$$

$$\rho C_p \left(v \frac{\partial \theta}{\partial r} + u \frac{\partial \theta}{\partial z} \right) = \kappa \nabla^2 \theta \quad (4.24)$$

At the inlet:

$$u = 1, \quad v = 0, \quad \theta = 1 \quad (4.25)$$

At the outlet:

$$\frac{\partial u}{\partial z} = 0, \quad v = 0, \quad \frac{\partial \theta}{\partial z} = 0 \quad (4.26)$$

At the wall of the tube:

$$u = 0, \quad v = 0, \quad \theta = 0 \quad (4.27)$$

4.5 FINITE ELEMENTS FORMULATION AND COMPUTATION

The Galerkin finite element method of Taylor and Hood (1973) and Dechaumphai (1999) is used to solve the governing equations along with boundary conditions for the considered problem. The equation of continuity has been used as a constraint due to mass conservation and this restriction may be used to find the pressure distribution. The finite element method is used to solve the Eqs. (4.21) - (4.27). The continuity equation is automatically fulfilled for large values of this penalty constraint. Then the velocity components (u, v), and temperature (θ) are expanded using a basis set. The Galerkin finite element technique yields the subsequent nonlinear residual equations. Three points Gaussian quadrature is used to evaluate the integrals in these equations. The convergence of solutions is assumed when the relative error for each variable between consecutive iterations is recorded below the convergence criterion ε such that $\psi^{n+1} - \psi^n \leq 10^{-4}$ where n is the number of iteration and ψ is a function of u, v or θ .

In finite element method, the mesh generation is the technique to subdivide a domain into a set of sub-domains, called finite elements, control volume etc. The discrete locations are defined by the numerical grid, at which the variables are to be calculated. It is basically a discrete representation of the geometric domain on which the problem is to be solved. The computational domains with irregular geometries by a collection of finite elements make the method a valuable practical tool for the solution of boundary value problems arising in various fields of engineering. Figure-4.0 displays the physical domain and it is solved by nonlinear solver.

Grid refinement test

In order to obtain grid independent solution, a grid refinement test was performed for the collapsible tube at respective values of $Re = 100$, $Pr = 0.71$, $Ha = 10$. Triangular mesh is used for two-dimensional simulation. The Figure (4.1) describes the satisfactory result of grid refinement test. In this problem, 5228 number of elements in collapsible tube is used. Using more number of elements is time consuming and effect on result is not significant.

Table 4.1: Grid sensitivity test (where $Re = 100$, $Pr = 0.71$, $Ha = 10$).

Elements	1444	2540	5228	15432
Nodes	9824	17095	34784	101537
Nu	0.565723	0.565577	0.565313	0.565154
θ_{av}	0.800965	0.800946	0.800934	0.800928
Time (s)	8.515	15.171	43.828	200.578

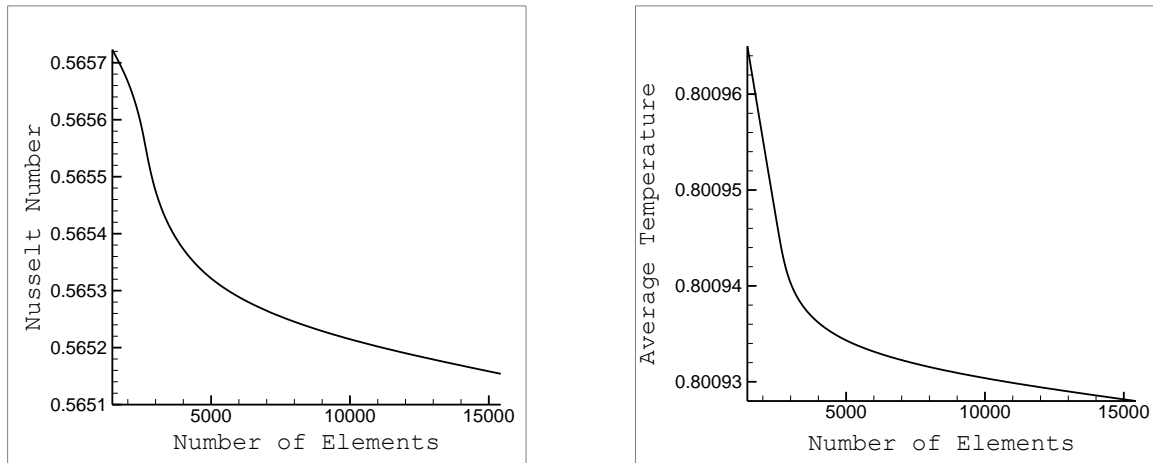


Figure 4.1 (a, b) : Nusselt number and Average Temperature versus mesh of the elements

4.6 RESULT AND DISCUSSION

Flow through axisymmetric collapsible tube has long been of interest to researcher. In this chapter, we focused on the effect of obstacle and the effect of magnetic field.

4.6.1 Velocity Profile of Collapsible Tube

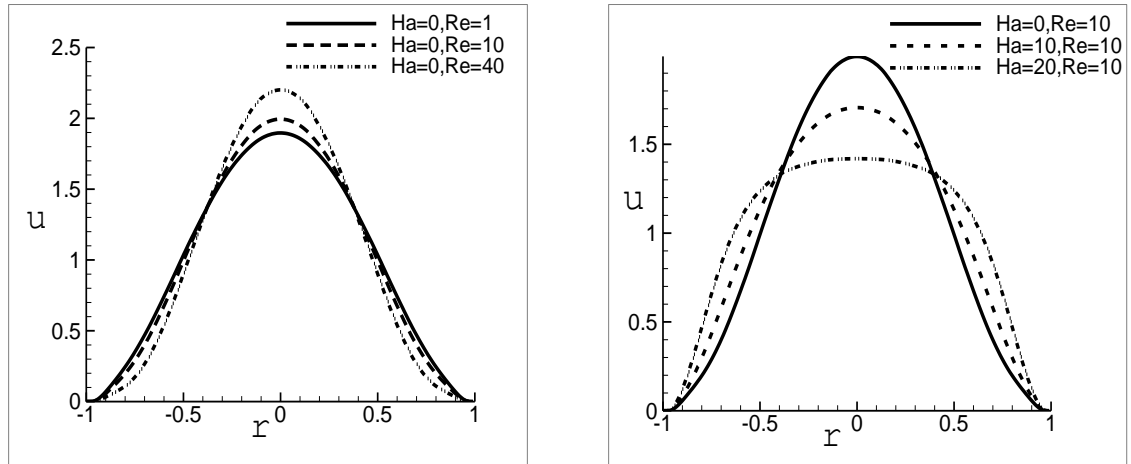


Figure 4.2 (a, b): Velocity versus radius of the tube for different Reynolds number and Hartmann number.

Figure 4.2 (a, b) illustrates the velocity versus radius of the collapsible tube. Velocity increases along the center line of the tube with the increases of Reynolds number. On the other hand, velocity decreases along the center line of the tube with increase of Hartmann number.

4.6.2 Effect of Obstacle on Collapsible Tube

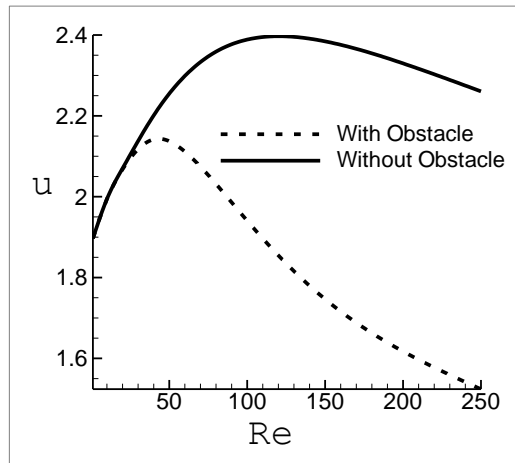


Figure 4.3: Velocity versus Reynolds number for obstacle and without obstacle.

Figure 4.3 illustrates the velocity versus Reynolds number in collapsible tube with obstacle and without obstacle. Velocity increases with the increase of Reynolds number. In collapsible tube with obstacle, velocity decreases at high Reynolds number for the creation of vortex. In

collapsible tube without obstacle, velocity increases with increase of Reynolds number. Whereas, very high Reynolds number, vortex is created at the collapsible wall that slightly reduces velocity.

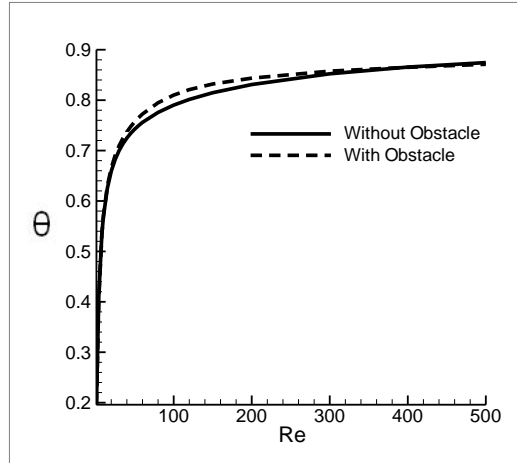


Figure 4.4: Temperature versus Reynolds number for obstacle and without obstacle at $Pr=0.71$.

Figure 4.4 illustrates the temperature versus Reynolds number in collapsible tube with obstacle and without obstacle. Reynolds number increases velocity that increases thermal convection. So, Reynolds number increases temperature. Presence of obstacle in the collapsible tube enhances the temperature.

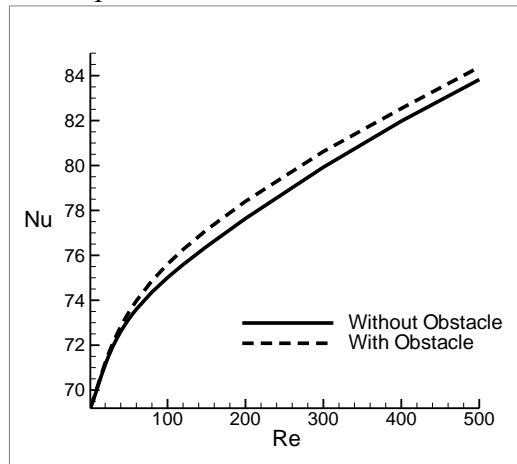


Figure 4.5: Rate of heat transfer versus Reynolds number for obstacle and without obstacle at $Pr=0.71$

Figure 4.5 demonstrates the Nusselt number versus Reynolds number in collapsible tube with obstacle and without obstacle. Reynolds number increases temperature that increases rate of heat transfer. Presence of obstacle improves the rate of heat transfer.

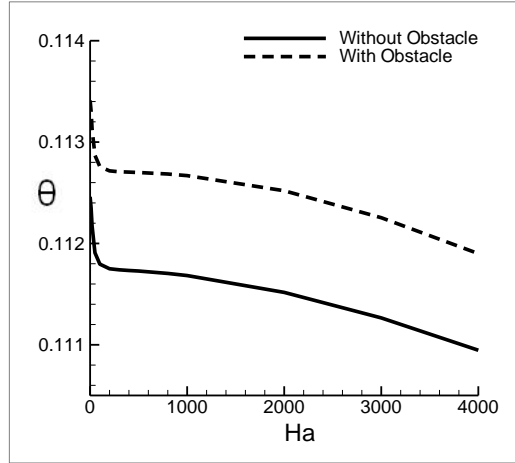


Figure 4.6: Temperature versus Hartmann number for obstacle and without obstacle at $Pr=0.71$

Figure 4.6 describes the temperature versus Hartmann number in collapsible tube with obstacle and without obstacle. Hartmann number creates an opposite flow that reduces thermal convection. So, increase of Hartmann number decreases the temperature. Presence of obstacle reduces the effect of Hartmann number on temperature.

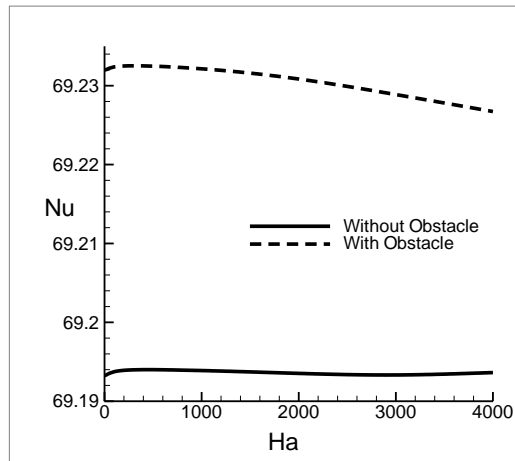


Figure 4.7: Rate of Heat transfer versus Hartmann number for obstacle and without obstacle at $Pr=0.71$ (Air)

Figure 4.7 displays the Nusselt number versus Hartmann number in collapsible with obstacle and without obstacle. Increase of Hartmann number slightly decreases the rate of heat transfer. Hartmann number decreases velocity and decreases thermal convection. So Hartmann number decreases temperature and rate of Heat transfer. Presence of obstacle increases rate of heat transfer in collapsible tube.

4.6.3 Effect of Hartmann Number on Heat Transfer

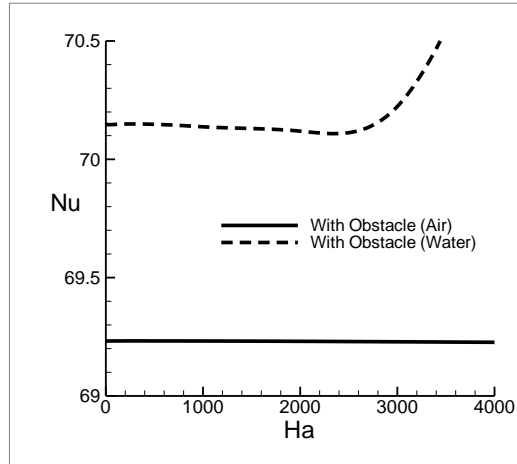


Figure 4.8: Rate of heat transfer versus Hartmann number with obstacle in air and water

Figure 4.8 shows the Nusselt number versus Hartmann number for two different fluids (Air, Water) with obstacle in collapsible tube. Hartmann number is more effective on highly viscous fluid. On Air, the effect of magnetic field is insignificant. On the other hand, on water, Hartmann number increases the rate of heat transfer drastically.

4.6.4 Effect of Reynolds Number on Temperature

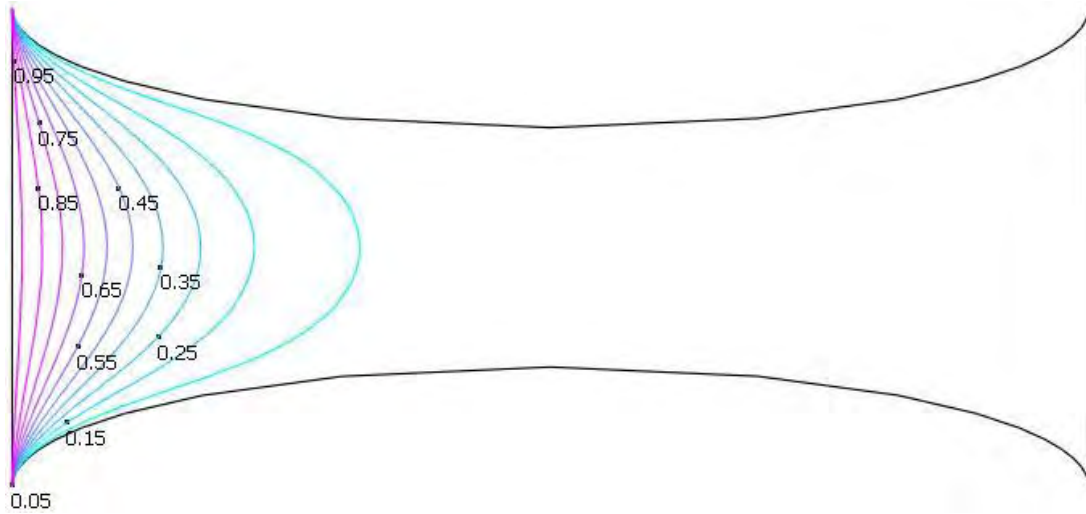


Figure 4.9 (a): Isothermal line on a collapsible tube without obstacle at $Re=1$.

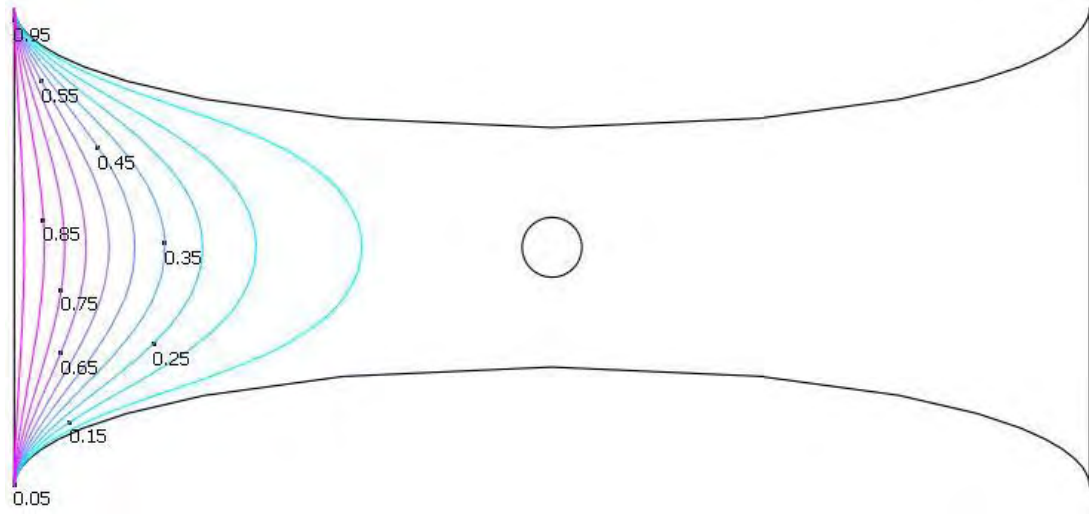


Figure 4.9 (b): Isothermal line on a collapsible tube with obstacle at $Re=1$.

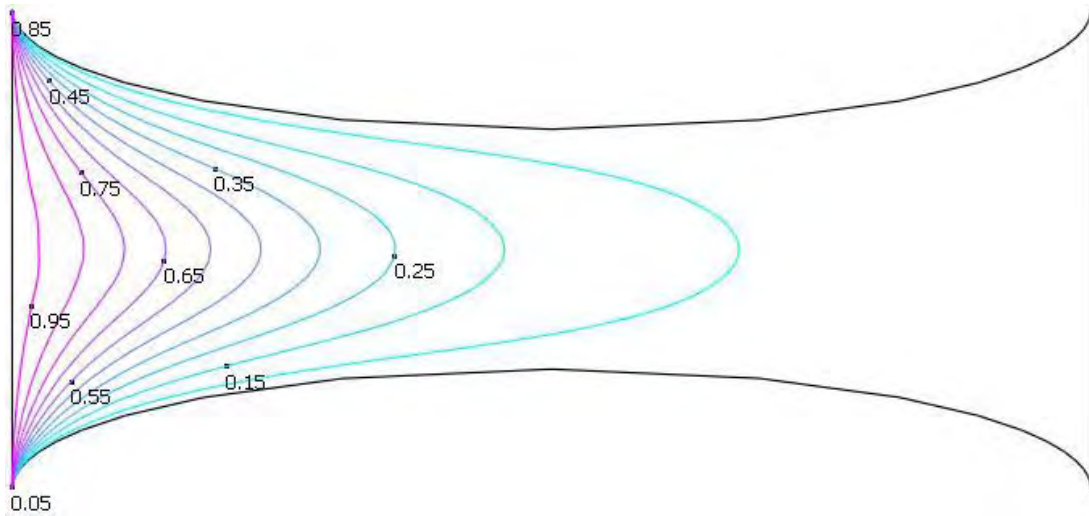


Figure 4.9 (c): Isothermal line on a collapsible tube without obstacle at $Re=10$.

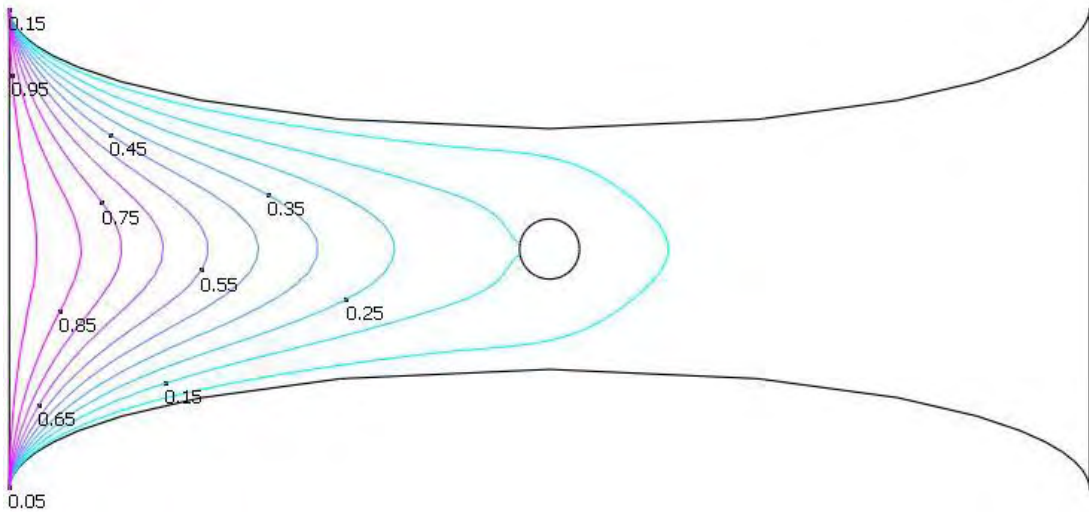


Figure 4.9 (d): Isothermal line on a collapsible tube with obstacle at $Re=10$.

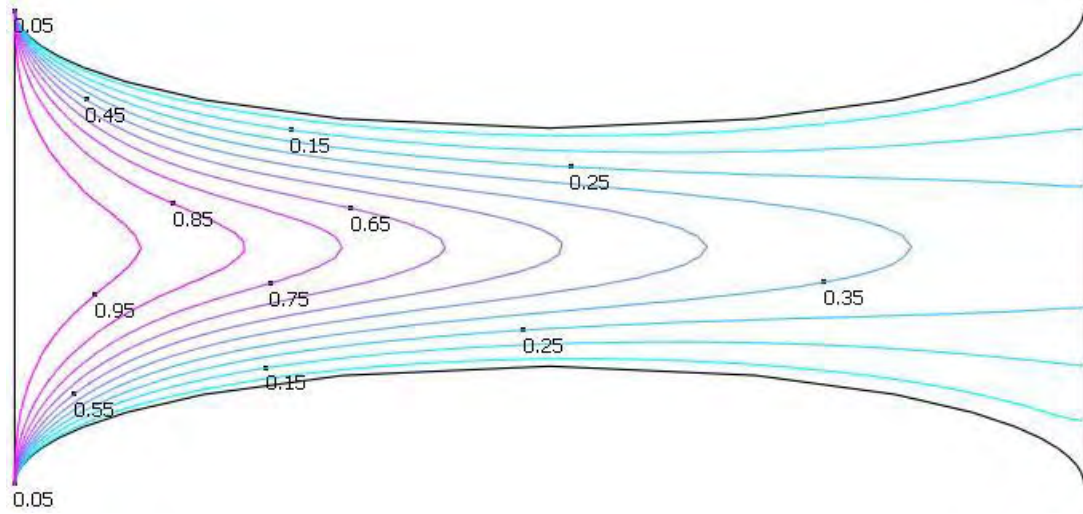


Figure 4.9 (e): Isothermal line on a collapsible tube without obstacle at $Re=40$.

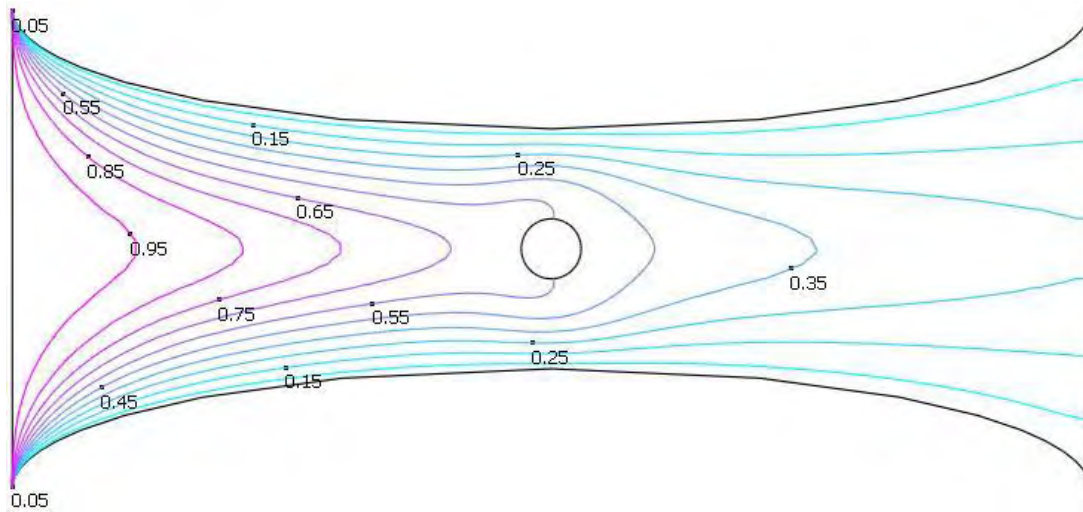


Figure 4.9 (f): Isothermal line on a collapsible tube with obstacle at $Re=40$.

Figure 4.9 displays the isothermal line on the collapsible tube for different Reynolds number. Increase of Reynolds number increases the intensity of isothermal line. However, the obstacle reduces the temperature of the tube.

4.6.5 Effect of Reynolds Number on Vortex

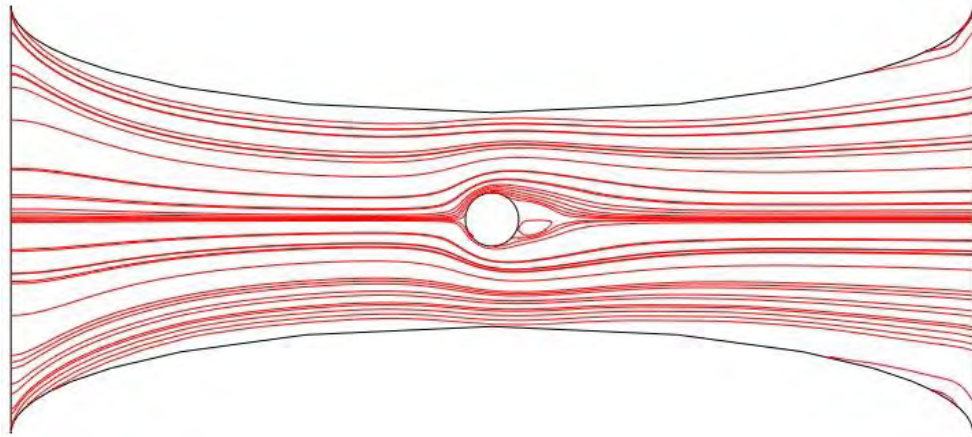


Figure 4.10 (a): Stream line on a collapsible tube with obstacle at $Re=100$.

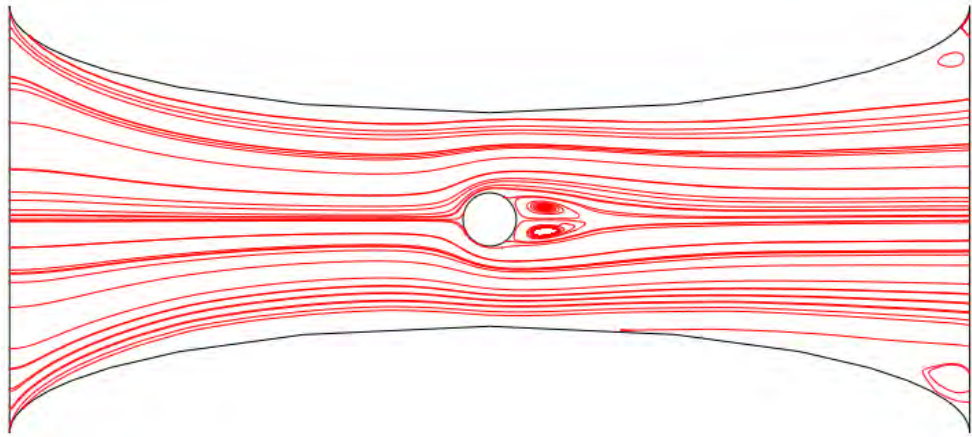


Figure 4.10 (b): Stream line on a collapsible tube with obstacle at $Re=200$.

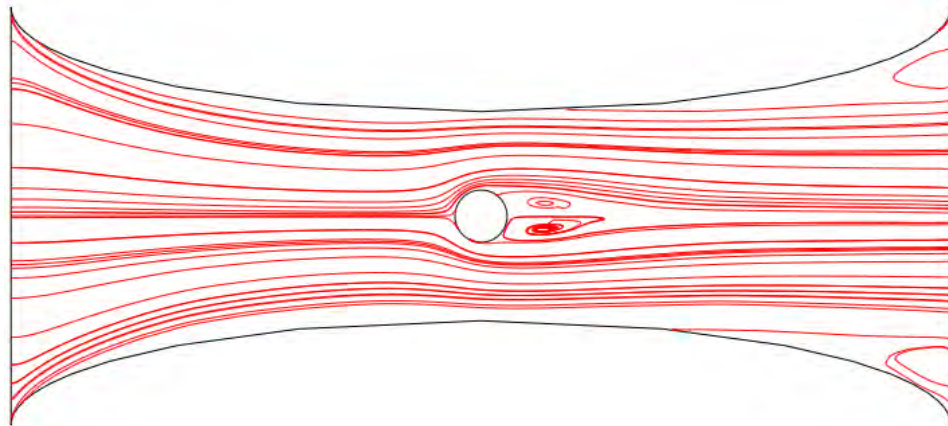


Figure 4.10 (c): Stream line on a collapsible tube with obstacle at $Re=300$.

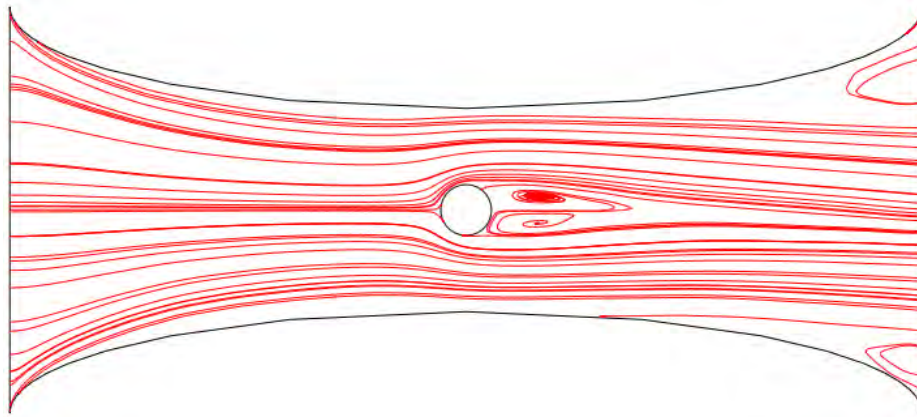


Figure 4.10 (d): Stream line on a collapsible tube with obstacle at $Re=400$.

Figure 4.10 displays the stream line around the vortex for different Reynolds number. Increase of Reynolds number increases the length of the vortex.

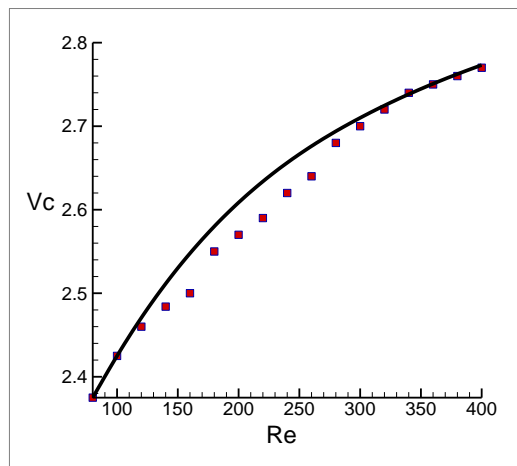


Figure 4.11: Vortex center distance from the obstacle versus Reynolds number

Figure 4.11 describes vortex center distance from the obstacle versus Reynolds number. The distance of the center of the vortex from the obstacle increases with increase of Reynolds number. On the other way, vortex center moves away from the obstacle due to increase of Reynolds number.

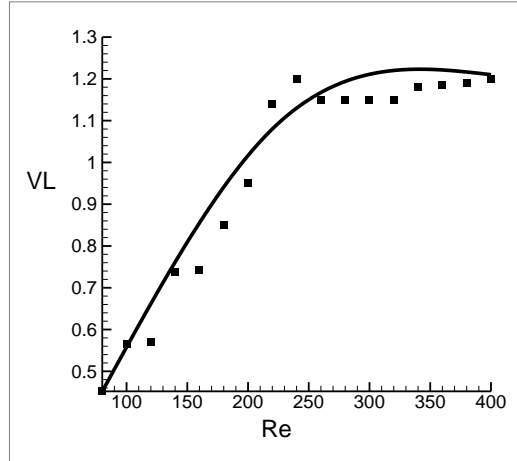


Figure 4.12: Vortex length from the obstacle versus Reynolds number

Figure (4.12) illustrates the vortex length versus Reynolds number. Vortex length increases with increase of Reynolds number.

4.6.6 Effect of Hartmann Number on Vortex

In this section, we describe how the small amount of Hartmann number diminishes the vortex. Here, we represent five picture of vortex around an obstacle to realize the magnetic effect.

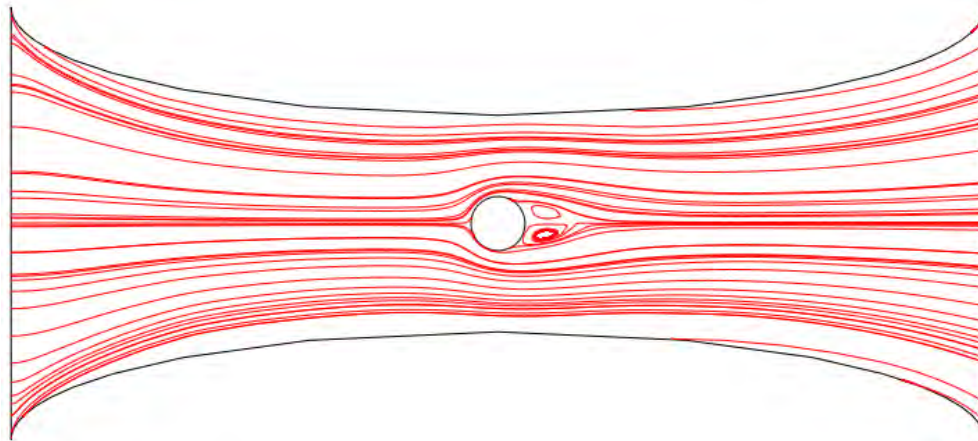


Figure 4.13 (a): Stream line on a tube with obstacle at $Re=400$, $Ha=0$.

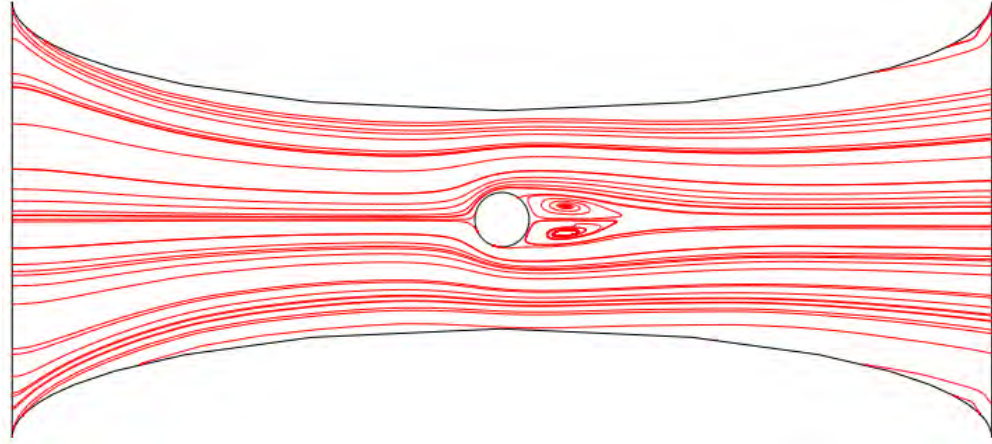


Figure 4.13 (b): Stream line on a tube with obstacle at $Re=400$, $Ha=20$.

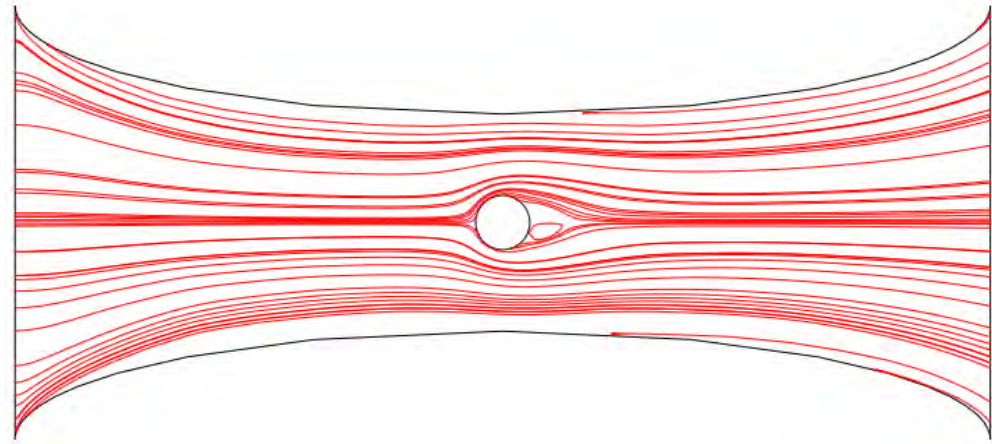


Figure 4.13 (c): Stream line on a tube with obstacle at $Re=400$, $Ha=40$.

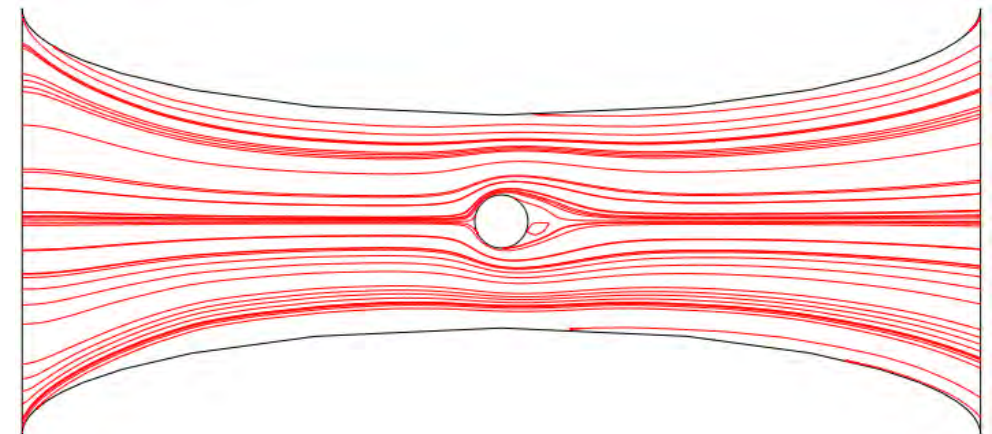


Figure 4.13 (d): Stream line on a tube with obstacle at $Re=400$, $Ha=60$.

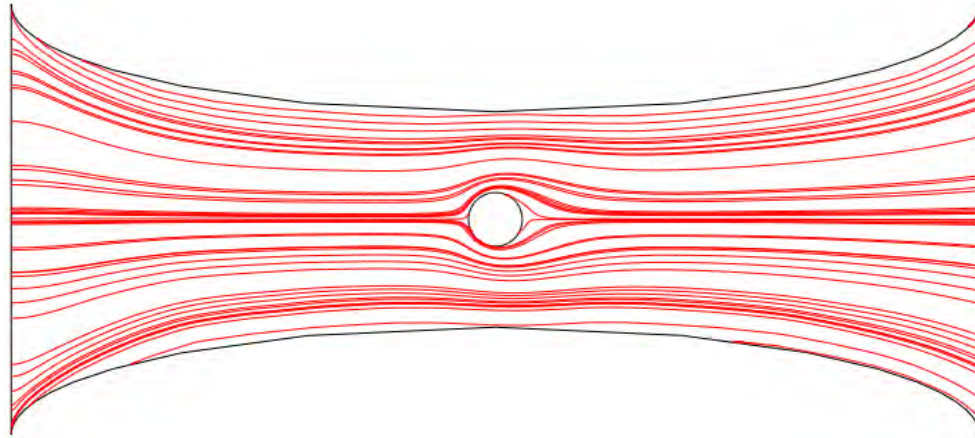


Figure 4.13 (e) : Stream line on a tube with obstacle at $Re=400$, $Ha=80$.

Figures (4.13) demonstrate the effect of Hartmann number on stream line for the fluid flow through a collapsible tube with obstacle. These figure shows the vortex is diminished by the increase of Hartmann number. Here, magnetic field is applied normal to the axis of the tube. Its effect acts at the opposite direction of velocity so it reduces the velocity and diminishes the size of the vortex.

In this section, we represent the effect of Hartmann number on vortex length and displacement of center of the vortex.

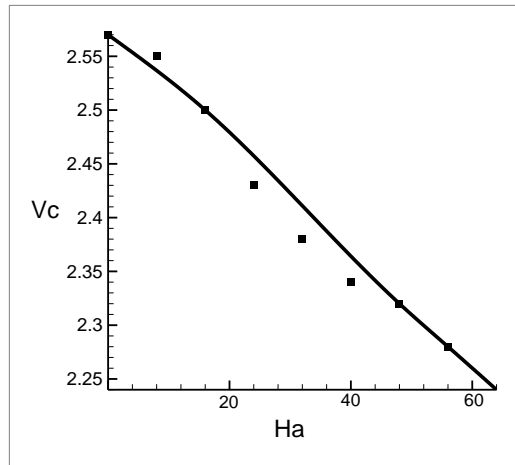


Figure 4.14: Vortex center distance from the obstacle versus Hartman number.

Figure (4.14) illustrates the vortex center distance from the obstacle versus Hartmann number. Vortex center distance decreases with increase of Hartmann number.

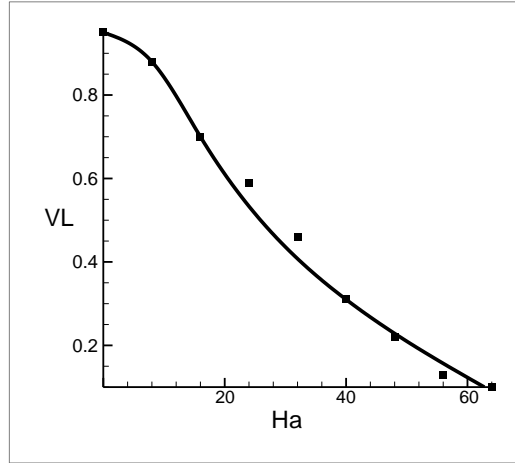


Figure 4.15: Vortex length from the obstacle versus Hartmann number.

Similarly, Figure 4.15 describes the vortex length from the obstacle versus Hartmann number. Vortex length decreases with increase of Hartmann number. The slope of the curve increases with increase of Hartmann number.

4.7 CONCLUSION

In this chapter, collapsible tube is represented with obstacle and magnetic field. The velocity and temperature of the tube varies with different dimensionless number in collapsible tube. The presence of obstacle and magnetic field change the velocity and temperature profile. The findings of this study are described below.

- 1) Temperature and rate of heat transfer increases with increase of Reynolds number.
- 2) Temperature and rate of heat transfer decreases with increase of Hartmann number.
- 3) Reynolds number increases the length of the vortex and it enhances the displacement of the center of vortex away from obstacle.
- 4) Hartmann number decreases the length of the vortex and it enhances the displacement of the center of the vortex towards the obstacle.

Chapter 5

CONCLUSION

In this thesis, analyze magneto-hydrodynamics with three different situations and investigate flow pattern, formation of vortex, profile of velocity and temperature, shear stress, flow stability and rate of heat transfer. In the 2nd chapter, the topic is MHD effect on wall driven flow and heat transfer through a porous tube where effect of magnetic field on flow stability is focused. Hartmann number decreases the critical Reynolds number, flow becomes unstable with the high intensity of magnetic field. However, Hartmann number increases the temperature and rate of heat transfer. In the 3rd chapter, the topic is MHD effect on fluid flow and heat transfer through a collapsible tube where magnetic field effect on stability of flow is focused. Critical Reynolds number of collapsible tube decreases with increases of magnetic effect. Magnetic field enhances the instability of this flow. However, temperature and rate of heat transfer increases with increase of Hartmann number. In the 4th chapter, the topic is MHD effect on fluid flow and heat transfer through collapsible tube with obstacle and without obstacle where effect of magnetic field and obstacle on stream line, isothermal line and vortex formation is focused. Reynolds number increases velocity, temperature and rate of heat transfer. In the presence of obstacle, Reynolds number increases the length of vortex and enhances the displacement of vortex. On the other hand, Hartmann number decreases velocity, temperature and rate of heat transfer. In the presence of obstacle, Hartmann number decreases the length of the vortex and enhances the displacement of vortex center towards the obstacle that diminishes the vortex in the flow.

Considering all topics, it is clear that Increase of Hartmann number decreases the velocity and Reynolds number increases temperature and rate of heat transfer. On the wall driven flow and collapsible tube, Hartmann number increases the scope of instability due to decrease of critical Reynolds number. On the collapsible tube with obstacle, Hartmann number reduces the vortex formation opportunity.

In this thesis, two separate methods such as finite element method and approximation method are used. The results of these two methods are not equal but similar. Here we discuss the main causes for this difference in the table below.

Approximation method	Finite elements method
Unsteady fluid flow is considered	Steady fluid flow is considered
Length of the tube is infinite	Length of the tube is fixed
Boundary condition is used for a circular cross section of the tube	Boundary condition is used for fixed inlet, outlet and two walls

That is why, we get similar pattern graphs from these two methods but the value of these graph results vary from one another.

Both methods are effective on different situations. Approximation method is very useful to determine the critical condition. This method sharply calculates the critical Reynolds number which indicates the stability of flow. Accuracy of approximation method depends on number of terms in the series. On the other hand, finite element method is very useful to determine the streamline, isothermal line of the problem. It is convenient for the irregular geometry and heterogeneous materials. Accuracy of the method depends on number of grid in the domain.

References

- Aradag, S. (2009), Unsteady Vortex Structure behind a Three Dimensional Turbulent Cylinder Wake, *Journal of Thermal Science and Technology*, 29(1), 91–98.
- Berman, A. S. (1953), Laminar flow in channels with porous walls, *J. Appl. Phys*, 24, 1232–1235.
- Bertram, C. D. and Pedley, T. J. (1982), A mathematical model of unsteady collapsible tube behaviour, *J. Biomech.*, 15, 39–50.
- Bertram, C. D. (1986), Unstable equilibrium behaviour in collapsible tubes, *J. Biomech.*, 19, 61–69.
- Bertram, C. D. Raymond, C. J. and Pedley, T. J. (1990), Mapping of instabilities for flow through collapsible tubes of deferring length, *J. Fluids. Struct.*, 4, 125–153.
- Bertram, C. D. and Raymond, C. J. (1991), Measurements of wave speed and compliance in a collapsible tube during self-excited oscillations: A test of the choking hypothesis, *Med. Biol. Eng. Comput.*, 29, 493–500.
- Bertram, C. D. Raymond, C. J. and Pedley, T. J. (1991), Application of nonlinear dynamics concepts to the analysis of self-excited oscillations of a collapsible tube conveying a fluid, *J. Fluids. Struct.*, 5, 391–287.
- Brower, R. W. and Scholten, C. (1975), Experimental evidence on the mechanism for the instability of flow in collapsible vessels, *Med. Biol. Engng*, 13, 839–845.
- Conrad, W. A. (1969), Pressure-flow relationship in collapsible tubes, *IEEE Trans. Bio Med.Engng*, 16, 284–295.
- Cowley, S. J. (1982), Elastic jumps in fluid-filled elastic tubes, *J. Fluid Mech.*, 116, 459–473.
- Cowley, S. J. (1983), On the wavetrains associated with elastic jumps on fluid-filled elastic tubes, *Q. J. Mech. Appl. Math.*, 36, 289–312.
- Dechaumphai, P. (1999), Finite Element Method in Engineering, 2nd ed., *Chulalongkorn University Press, Bangkok*.
- Domb, C. and Sykes, M. F. (1957), On the susceptibility of a ferromagnetic above the Curie point, *Proc. R. Soc. Lond. Ser. A*, 240, 214–228.
- Drazin, P. G. and Tourigny, Y. (1996), Numerical study of bifurcations by analytic continuation of a function defined by a power series, *SIAM J. Appl. Math.*, 56, 1–18.

- Elad, D. Kamm, R. D. and Shapiro, A. H. (1987), Choking phenomena in a lung-like model, *ASME J. Biomech. Engng*, 109, 1–9.
- Flaherty, J. E. Keller, J. B. and Rubinow, S. I. (1972), Post buckling behaviour of elastic tubes and rings with opposite sides in contact, *SIAM J. Appl. Math.*, 23, 446 – 455.
- Grotberg, J. B. (1971), Pulmonary flow and transport phenomena, *Ann. Rev. Fluid Mech.*, 26, 529–571.
- Guttamann, A. J. (1989), Asymptotic analysis of power–series expansions, Phase Transitions and Critical Phenomena, C. Domb and J. K. Lebowitz, eds. *Academic Press, New York*, 1–234.
- Heil, M. (1997), Stokes flow in collapsible tubes-computational and experiment, *J. Fluid Mech.*, 353, 285–312.
- Hunter, D. L. and Baker, G. A. (1979), Methods of series analysis III: Integral approximant methods, *Phys. Rev. B*, 19, 3808–3821.
- Hunter, C. and Guerrieri, B. (1980), Deducing the properties of singularities of functions from their Taylor series coefficients, *SIAM J. Appl. Math.*, 39, 248–263.
- Kays, W. M. and Crawford, M. E. (1993), Convective heat and mass transfer. *Mcgraw-Hill Inc.*
- Makinde, O. D. (1995), Laminar flow in a channel of varying width with permeable boundaries, *Rom. Jour. Phys.*, 40(4–5), 403.
- Makinde, O. D. (1996), Computer extension and bifurcation study by analytic continuation of porous tube flow, *Jour. Math. Phys. Sci.*, 30, 1–24.
- Makinde, O. D. (1999), Extending the utility of perturbation series in problems of laminar flow in a porous pipe and a diverging channel, *Jour. of Austral. Math. Soc. Ser. B*, 41, 118–128.
- Makinde, O. D. (2001), Heat and mass transfer in a pipe with moving surface: Effects of viscosity variation and energy dissipation, *Quaestiones Mathematicae*, 24, 97–108.
- Makinde, O. D. Motsumi, T. G., and Ramollo, M. P., (2002), Squeezing flow between parallel plates: A bifurcation study, *Far East Jour. Appl. Math.*, 9(2), 81–94.
- Makinde, O. D. (2005), Collapsible tube flow: a mathematical model, *Rom. Journ. Phys.*, 50(5-6), 493–506.
- Makinde, O. D. Aregbesola, Y.A.S., and Odejide, S.A., (2006), Wall driven steady flow and heat transfer in a porous tube, *Kragujevac J. Math.*, 29, 193–201.

- Makinde, O. D. (2009), Hermite-Pade approach to thermal radiation effect on inherent irreversibility in a variable viscosity channel flow, *Computers and Mathematics with Applications*, 58(11-12), 2330–2338.
- Mathelin, L. Bataille, F. and Lallemand, A. (2005), Near Wake of a Circular Cylinder Submitted to Blowing – I Boundary Layers Evolution, *International Journal of Heat and Mass Transfer*, 44, 3701–3708.
- Munson-McGee, S. H. (2002), An approximate analytical solution for the fluid dynamics of laminar flow in a porous tube, *Journal of Membrane Science*, 197, 223–230.
- Norberg, C. (1987), Effects of Reynolds Number and a Low-Intensity Free Stream Turbulence on the Flow around a Circular Cylinder, *Chalmers University of Technology*, ISSN 02809265.
- Odejide, S.A. and Aregbesola, Y.A.S. (2006), Wall driven steady flow and heat transfer in a tube, *International Journal of Pure and Applied Mathematics*, 24(32005), 323–330.
- Odejide, S.A. Aregbesola, Y.A.S. and Makinde, O.D. (2008), Fluid flow and heat transfer in a collapsible tube, *Rom. Journ. Phys.*, 53(3-4), 499–506.
- Reddy, M. G. Reddy, N. B. and Reddy, B. R. (2009), Unsteady MHD convective heat and mass transfer flow past a semi-infinite vertical porous plate with variable viscosity and thermal conductivity, *Int. J. Appl. Math and mech.*, 5(6), 1–14.
- Sellar, J. R. (1955), Laminar flow in channel with porous wall at high suction Reynolds number, *J. Appl. Phys*, 26, 489–490.
- Sergeev, A. V. (1986), A recursive algorithm for Padé–Hermite approximations, *U.S.S.R. Comput. Math. Phys.*, 26, 17–22.
- Sergeev, A. V. and Goodson, A. Z. (1998), Summation of asymptotic expansions of multiple valued functions using algebraic approximants application to an harmonic oscillators, *J. Phys., A: Math. Gen.*, 31, 4301–4317.
- Shafer, R. E. (1974), On quadratic approximation, *SIAM J. Numer. Anal.*, 11, 447–460.
- Taylor, C. and Hood, P. (1973), A numerical solution of the Navier-Stokes equations using finite element technique, *Computer and Fluids*, 1, 73-89.
- Yuan, S. W. and Finkelstein, A. B. (1956), Laminar pipe flow injection and suction through a porous wall, *Trans. ASME* ,78, 719–724.